Climate Services 33 (2024) 100426

Contents lists available at ScienceDirect

Climate Services

journal homepage: www.elsevier.com/locate/cliser

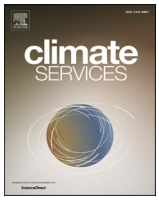

Sub-regional variability of residential electricity consumption under climate change and air-conditioning scenarios in France

Qiqi Tao [a,*], Marie Naveau [a], Alexis Tantet [a], Jordi Badosa [a], Philippe Drobinski [a]

[a] Laboratoire de Météorologie Dynamique – Institut Pierre-Simon Laplace, Ecole Polytechnique – Institut Polytechnique de Paris, Ecole Normale Supérieure – PSL Université, Sorbonne Université, CNRS, Palaiseau 91128, France

ARTICLE INFO

Keywords:
Residential electricity consumption
Cooling demand
Climate change impacts

ABSTRACT

The residential sector is important for the energy transition to combat global warming. Due to the geographical variability of socio-economic factors, the highly dependent residential electricity consumption (REC) should be studied locally. This study aims to project future French REC considering climate change and air-conditioning (AC) scenarios and to quantify its spatial variability. For this purpose, a linear temperature sensitivity model fitted by annual observed electricity consumption data and historical temperature is applied at an intra-regional scale. Future temperature-sensitive REC is computed by applying the model to temperature projections under the climate change pathway RCP8.5. Three AC scenarios are considered: (1) A 100% AC rate scenario assuming that any region partially equipped with AC systems nowadays will have all its households equipped with AC, but local temperature sensitivity will no longer progress; (2) A gradual spreading scenario mimicking "do like my neighbor" behavior; (3) A combination of the two scenarios. Increasing temperatures lead to an overall REC decrease (−8 TWh by 2040 and down to −20 TWh by 2100) with significant spatial variability, which had never been quantified and mapped due to a lack of suited methodology and limited available data at the finest scale. The evolution of REC is modulated by the evolution of cooling needs and the deployment of AC systems to meet those needs. In the first 2 AC scenarios, the decrease of REC due to climate change could be totally offset in the South of France, which would then display an increase in REC. When the 2 AC scenarios are combined, an increase in REC could be seen over the whole country. The most extreme AC scenario shows a potential REC rise due to AC usage by 2% by 2040 and even 32% by 2100, which could be canceled by increasing the cooling setpoint up to 26–27 °C.

Practical implications

The residential sector is the leading electricity consumer in France, representing more than one-third of the final electricity uses. This sector has therefore to implement a pathway to reduce energy demand and greenhouse gas emissions. The relevance of related policies depends on the expected change in residential electricity consumption (REC) for various climate change scenarios and user behavior. REC change in climate change scenarios has already been studied at the country scale, but important physical (e.g. local weather conditions) and socio-economic (revenue, air-conditioning use, etc.) determinants of REC display a large spatial variability which implies REC should be studied locally.

The REC model is computed using a linear temperature sensitivity model fitted by annual observed electricity consumption data and daily temperatures applied at the smallest French geographic census unit named Ilots Regroupés pour l'Information Statistical (IRIS), which divides the territory into meshes of about 2000 inhabitants per unit cell. Once the current electricity sensitivity is fitted for each IRIS, the REC change is computed by applying the model to temperature projections under climate change scenario RCP8.5 at intermediate (2025–2055) and far (2070–2100) time horizons based on 5 climate simulations performed in the frame of the international CORDEX program. In addition, two cooling scenarios based on the air-conditioning adoption rate and the cooling temperature sensitivity are also investigated.

When only climate change is considered, REC is projected to decrease with decreasing heating needs in most IRIS cells. However, because of already deployed cooling equipment, REC is expected to

* Corresponding author.
E-mail address: qiqi.tao@hotmail.com (Q. Tao).

https://doi.org/10.1016/j.cliser.2023.100426

Available online 3 December 2023

increase in 3–7% of the territory, totally offsetting the effect of reduced heating needs. A larger variability is found within administrative regions, including a few hundred to thousands of IRIS, than between administrative regions. Including AC scenarios offset in part the REC negative trend, with REC projected to increase in the South-East in the most conservative scenario to nearly the entire territory when large spreading and rate of AC use are assumed. Large AC use may lead to REC change ranging from 2% by 2040 to 32% by 2100, contributing to enhanced greenhouse gas emission and the urban heat island effect.

Such results call for targeted and local information actions where the risk of spreading is high to limit the spreading and rate of use or mitigate their effect with more energy-efficient AC systems. As our projected future climate in Southern France is similar to the present climate of countries more to the South, which has not seen a large deployment of AC equipment, analyzing the socio-economic drivers, the energy policies of these countries and drawing inspiration from them to deploy locally adapted actions should be considered. Also, adapting the cooling setpoint could help elaborate energy policies to lower the cooling temperature-sensitive REC. Based on our model, shifting the cooling setpoint from 21 °C at present to 23–24 °C by 2040 and 26–27 °C by 2085 would prevent any cooling REC rise in our worst-case scenarios. These values are consistent with existing recommendations (e.g. US DoE). Finally, low-tech alternative solutions, such as cool white roof coating widely implemented in subtropical regions, can be implemented in France to improve the thermal comfort of buildings and reduce the use of AC equipment and their impact on the environment.

1. Introduction

France is committed, with the energy transition law for green growth of 2015, to reducing its greenhouse gas emissions by 40% by 2030 and divided by four by 2050. It also plans to reduce its consumption of fossil fuels by 30% by 2030 and to halve its final energy consumption in 2050 compared to 2012 (regulations passed under the *Law for the ecological transition and green growth*[1]). This regulation contributes to the *Paris climate agreement*[2] to keep temperature increases well below 2 °C and to pursue efforts for 1.5 °C. The French residential sector represents 20% of the CO2 emission of the country and 30% of the final energy uses. Hence, this sector could be a significant opportunity and challenge for policies to combat global warming. Indeed, the law text emphasizes improving building energy efficiency, thermal renovation of buildings, and constructing buildings with high energy performance.

Limiting electricity consumption in the residential sector through actions aimed at improving the energy performance of buildings is therefore a major environmental challenge for communities. However, residential electricity consumption (REC) is highly dependent on household income, the thermal quality of occupied dwellings, and the cost of energy with regard to the purchasing power of the households (Giraudet et al., 2012; Branger et al., 2015; Frederiks et al., 2015) and therefore displays a very large spatial variability, especially in urban areas which are characterized by the heterogeneity of their demographic, socio-economic, environmental and cultural characteristics (Li and Kwan, 2018; Pickett et al., 2017) underlying urban resource demands (Rosales and Worrell, 2018; Voskamp et al., 2020). The case of France has been investigated specifically and supports studies conducted in other countries (Lévy and Belaïd, 2018).

Electricity demand also depends on the outdoor temperature. Demand for cooling rises once the temperature exceeds a cooling setpoint, while electricity demand for heating grows once the temperature drops below a heating setpoint (Petrick et al., 2010; Auffhammer and Mansur, 2014; Damm et al., 2017; Wenz et al., 2017; Kozarcanin et al., 2019). As a result, a theoretical U-shaped link exists between electricity demand and temperature. Choices made by individuals to utilize heating and cooling systems to maintain a comfortable temperature in their residences directly impact electricity demand (Emodi et al., 2018; Emenekwe and Emodi, 2022). Substantiated correlations between consumption and climate and weather conditions (Meng et al., 2020), demographic and economic factors (Bettignies et al., 2019) and urban and architectural morphological characteristics (Chen et al., 2020; You and Kim, 2018) cause the large spatial variability in residential energy demand. Climate, socio-economic and morphological characteristics have proven explanatory variables for energy demand and its spatial pattern (Chen et al., 2020; Kennedy et al., 2015; Wiedenhofer et al., 2013).

The link between temperature and electricity demand has been studied using various models [e.g. (Narayan et al., 2007; Emodi et al., 2018)]. One approach is to model this nonlinear relationship by a smooth but nonlinear function of the temperature. For instance, Moral-Carcedo and Vicéns-Otero (2005) and Damm et al. (2017) used a Logistic Smooth Transition (LSTR) function to model the electricity demand response to temperature variations in European countries. The advantage of such a model is that it adequately captures the rather smooth response of electricity demand summed over a large domain to temperature variations. On the other hand, it is less straightforward to interpret the physical meaning of the parameters of such a model. Another approach is to model the electricity demand as a linear combination of nonlinear functions of the temperature (making it a generalized linear model). For instance, Sailor and Muñoz (1997) studied the monthly electricity and gas consumption for states in the US using a linear model with degree-day (DD) inputs in addition to wind speed and relative humidity.

In France, outdoor temperature increase could reach up to 3.8 °C by 2100 with regards to 1900–1930 if no policy is in place to reduce greenhouse gas emissions (Ribes et al., 2022). Pilli-Sihvola et al. (2010) have investigated the impact of climate change using the DD approach on building energy demand for heating and cooling and the associated energy cost using climate simulations of the 3rd Coupled Model Intercomparison Project (CMIP3). More recently, Larsen et al. (2020) find in downscaled CMIP5-climate simulations that when temperature evolution is considered as the only factor of change, needs for cooling increase by 33% to 204% between 2050 and 2010 and needs for heating decrease by −31% to −6% while Damm et al. (2017) predict the impact of a +2 °C global temperature change on European electricity demand, with for France, an estimated decrease in total electricity consumption between -10TWh and -16TWh. The optimistic reduction in electricity projection is due to France's current heating-dominated state. All households in the country utilize specific heating systems such as gas, oil, wood, or district heating, among which 37% employ electric heating. In contrast, the national adoption of air-conditioning (AC) remains relatively low, standing at only approximately 22% when considering all types and sizes of air conditioners, including mobile and heat pump units.

Rising temperatures and temperature extremes, in particular, imply increased use of air conditioners, both in hot and humid emerging economies where incomes are rising and in industrialized economies where consumer expectations in terms of thermal comfort are constantly growing (van Ruijven et al., 2019). Previous studies (van Ruijven et al., 2019; ?; ?) suggest that climatic conditions will encourage more households to adopt AC systems, therefore affecting electricity expenditures. On a global scale, the final energy consumption for AC in residential and commercial buildings has more than tripled between 1990 and 2016. The share of cooling in REC increased from around 2.5% to 6% during the same period. The use of AC equipment is expected to increase dramatically, becoming one of the main drivers of global electricity demand (International Energy Agency, 2018).

In France, as heat waves are more and more frequent and long, many households and businesses are equipped with AC for more comfort (Lemonsu et al., 2015). In 2020, for the first time, the number of equipment sold exceeded 800,000 units, whereas it had stabilized at

[1] https://www.legifrance.gouv.fr/loda/id/JORFTEXT000031044385
[2] https://unfccc.int/sites/default/files/english_paris_agreement.pdf

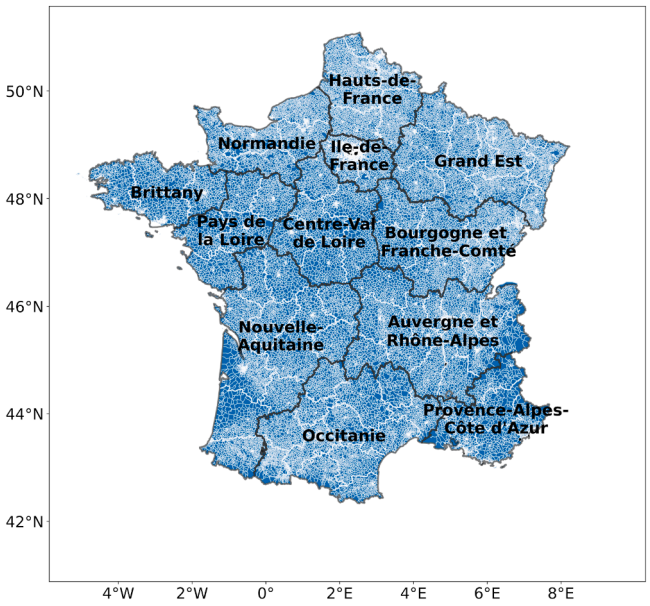

Fig. 1. Map of 12 administrative regions of metropolitan France, with thicker white lines representing 94 departments and thinner white lines representing more than 48000 IRIS cells. (Plate carrée projection, same projection used in the presented study).

around 350,000 per year previously. In 2020, 25% of individuals are equipped compared to 14% in 2016, with disparities linked to the type of dwelling (31% of owners of individual houses compared to 20% of households living in collective housing), socio-professional category (37% of liberal professions, executives and higher intellectual professions against only 19% of households whose reference person is unemployed or inactive) and place of residence (e.g. 47% of inhabitants of the South-East and Corsica against only 11% in Brittany) (ADEME, CODA STRATEGIES, 2021).

However, most previous studies of future consumption projection only focus on continental and national scales while not considering the sub-national disparity of temperature changes and non-climatic factors listed above. We aim to fill this gap by examining whether the national results proposed by these earlier studies remain consistent at smaller scales, given that changes in consumption and geographical variations in adaptation can lead to inequalities. We provide valuable information on the local impacts of climate change and building cooling strategies on residential energy demand, which can aid local climate and energy planning and decision-making. Specifically, we focus on the sub-regional variability of changes in residential AC requirements for cooling needs in the context of climate change. To this end, we use a modified temperature sensitivity model to project future REC at a fine scale. The smallest geographic scale used in this study is the so-called Ilots Regroupés pour l'Information Statistical (IRIS), here referred to as cells, which divides the French territory into a collection of about 2000 inhabitants per cell. These cells are defined by respecting geographic and demographic criteria and have recognizable contours without ambiguity and stability over time. France has a total of 50,800 cells (IGN, 2009). In metropolitan France, these cells are distributed among 12 administrative regions represented in Fig. 1. This model is designed to distinguish between different aspects of electricity use using data from all residential buildings, irrespective of their heating or cooling equipment. The projection of future residential electricity consumption is based on climate change pathway RCP8.5, using downscaled CMIP5 climate simulations carried out as part of EURO-CORDEX (Jacob et al., 2014) and MEC-CORDEX (Ruti et al., 2016), while considering different scenarios of AC use for cooling - full generalization or saturation.

After the introduction in Section 1, the details of the model can be found in Section 2, with information about the temperature and REC data that are applied to fit the model as inputs for the case of France and the future temperature projection and AC use scenarios. REC projection results and discussion are presented in Section 3, and the conclusion and policy implications are given in Section 4. The global flow chart of the total work is shown in Fig. 2.

2. Methodology and data

In this section, we explain how the REC is projected at the sub-communal scale by applying a temperature sensitivity model trained on historical data to climate projections. We also present the data for the application to France and define the scenarios used as projections of AC use with widespread adoption or saturation cases.

2.1. Temperature sensitivity statistical model

The relationship between the surface air temperature and the energy consumption over a domain is what we call the temperature sensitivity of the consumption. It has been modeled in various ways as presented in the previous section. The advantages of the DD approach are that it is simple to implement as a linear regression model with standard machine learning software and that it is straightforward to interpret the coefficients of the models as temperature sensitivities. For these reasons, we follow the DD approach in this study. The heating degree-days (HDD) (resp. the cooling degree-days (CDD)) for a domain is a positive quantity computed from data for the (weighted-) average temperature of the domain. It is given by the sum over a period of the degrees below (resp. above) a certain setpoint temperature per timestep. Here, the timestep d is a day and the period y a year between 2011 and 2018 (included),

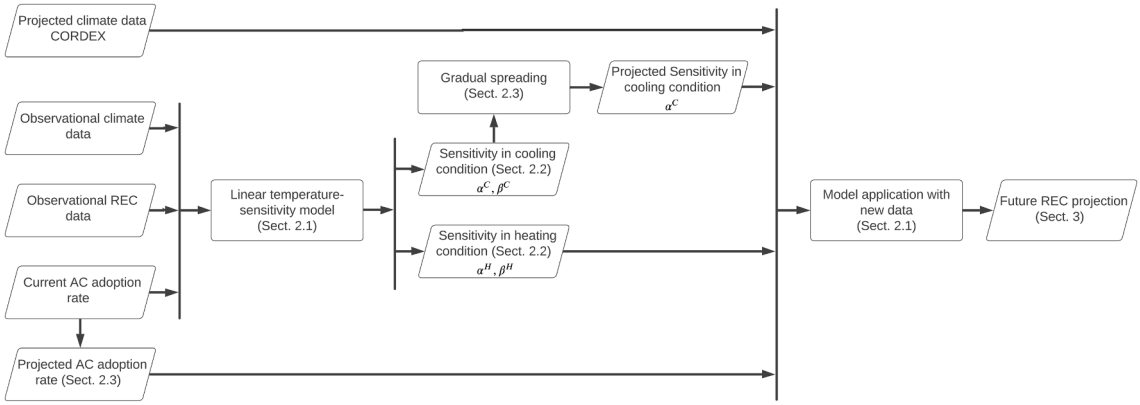

Fig. 2. Flow chart of the present study.

Table 1
Summary of variables and their physical meanings presented in Eq. 2.

Variable	Meaning
$E_i(y)$	Annual REC normalized by surface for cell i and year y (kWh/ m^2)
B_i	The basic daily REC for cell i (kWh/ m^2)
N_y	The number of days in a year y (365 or 366)
α_i^{H}	Heating temperature sensitivity for cell i (kWh/ (DD m^2))
α_i^{C}	Cooling temperature sensitivity for cell i and year (kWh/ (DD m^2))
$\eta_i^{\mathrm{El}}(y)$	Rate of electric heating for cell i and year y (%)
$\eta_i^{\mathrm{AC}}(y)$	Rate of AC adoption for cell i and year y (%)
$\beta_i^{\mathrm{H}}(y)$	Coefficient measuring increase in yearly REC per HDD and unit of area for cell i and year y (kWh/ (DD m^2))
$\beta_i^{\mathrm{C}}(y)$	Coefficient measuring increase in yearly REC per CDD and unit of area for cell i and year y (kWh/ (DD m^2))

while different domains, or cells, i are considered, each corresponding to a different IRIS. The HDD and CDD are thus defined here as (Moral-Carcedo and Vicéns-Otero, 2005),

$$\begin{aligned}\mathrm{HDD}_i\left(y\right) &:= \sum_{d=1}^{N_y} \max\left(0; T_i^H - T_i\left(y,d\right)\right)\\ \mathrm{CDD}_i\left(y\right) &:= \sum_{d=1}^{N_y} \max\left(0; T_i\left(y,d\right) - T_i^C\right),\end{aligned} \tag{1}$$

where $T_i(y,d)$ is the daily-mean surface air temperature for a day d of year y averaged over cell i, T_i^H and T_i^C with $T_i^C \geqslant T_i^H$ are respectively the heating and cooling setpoints for cell i, and N_y (365 or 366) is the number of days in year y. The heating and cooling setpoints T_i^H and T_i^C are parameters to be estimated.

The REC scales with the living area in each cell. To leave out this factor, we divide the REC by the living area, giving the normalized annual REC $E_i(y)$ for cell i and year y in kWh/ m^2. For a given scenario (see Section 2.3), the general temperature sensitivity model is then expressed as,

$$\begin{aligned}E_i(y) &= \beta_i^{\mathrm{H}}(y)\mathrm{HDD}_i(y) + B_i N_y + \beta_i^{\mathrm{C}}(y)\mathrm{CDD}_i(y)\\ &= \alpha_i^{\mathrm{H}}\eta_i^{\mathrm{El}}(y)\mathrm{HDD}_i(y) + B_i N_y + \alpha_i^{\mathrm{C}}\eta_i^{\mathrm{AC}}(y)\mathrm{CDD}_i(y).\end{aligned} \tag{2}$$

.

The first equation in (2) relates $E_i(y)$ to a heating, a basic, and a cooling REC (from left to right). The basic daily REC B_i (kWh/ m^2) is part of the REC that does not depend on temperature. It determines the REC fully when $T_i^H \leqslant T_i(y,d) \leqslant T_i^C$. In this study, we focus on the effect of climate change and the rate of air-conditioning (AC) adoption on the REC. Factors affecting the basic REC are thus assumed to remain fixed so that B_i does not depend on time. The temperature-sensitive RECs for a given year are proportional to DD. The coefficients of proportionality $\beta_i^{\mathrm{H}}(y)$ and $\beta_i^{\mathrm{C}}(y)$ (kWh/ (DD m^2)) measure the increase in yearly REC per DD and unit of area in cell i. Each cell includes residential buildings with and without electric appliances. Thus, other things remain the same, lowering the fraction η_i^{El} of residential buildings in cell i with electric heating lowers β_i^{H}. To estimate the temperature-sensitive electric consumption restricted to residential buildings with electric heating, β_i^{H} is developed as the product of η_i^{El} with the heating temperature sensitivity α_i^{H} (kWh/ (DD m^2)) of cell i. Factors affecting the heating temperature sensitivity (consumer behavior, thermal efficiency of residential buildings, etc.) are also assumed to remain fixed so that α_i^{H} is independent of time.

However, the rate of electric heating η_i^{El} may vary in time. Yet, the data used in this study only provides estimates of η_i^{El} for the year 2018 (Section 2.2.1). We therefore assume that this rate is fixed to that of 2018, $\eta_i^{\mathrm{El}}(y) = \eta_i^{\mathrm{El}}(2018) := \eta_i^{\mathrm{El}}$, and so $\beta_i^{\mathrm{H}}(y) = \beta_i^{\mathrm{H}}(2018)$, for all years and all cells. This implies that an Ordinary Least-Squares (OLS) regression with β_i^{H} as coefficient and $\mathrm{HDD}_i(y)$ as input is equivalent to an OLS regression with α_i^{H} as coefficient and $\eta_i^{\mathrm{El}}\mathrm{HDD}_i(y)$ as input. Similarly, β_i^{C} is developed as the product of the fraction η_i^{AC} of residential buildings in cell i equipped with AC with the cooling temperature sensitivity α_i^{C} (kWh/ (DD m^2)) of cell i. Note, however, that while all residential buildings include some form of heating so that η_i^{El} reflects the choice of heating system, all AC systems are electric, and η_i^{AC} gives the adoption rate of AC equipment. Regarding η_i^{AC}, as presented in the previous section, the AC adoption rate has increased during the past several years and hence depends on the year during the training (Section 2.2.4). For future projection, both α_i^{C} and η_i^{AC} vary with the choice of AC use scenario, but they are assumed constant during a given period (Section 2.3.2).

In summary, all the parameters with their physical meanings are given in Table 1. For all pairs (i,y) of cells i and years y, the model inputs are.

- $\eta_i^{\mathrm{El}}(y)\mathrm{HDD}_i(y)$ and
- $\eta_i^{\mathrm{AC}}(y)\mathrm{CDD}_i(y)$,

where $\mathrm{HDD}_i(y)$ and $\mathrm{CDD}_i(y)$ depend on the daily-mean temperatures $T_i(y,d)$ for all days d in y. The model coefficients are the temperature sensitivities α_i^{H} and α_i^{C} and the hyperparameters are T_i^H and T_i^C. The total number of cells is assumed to remain fixed. In the following sections, we present how this model is trained and applied to climate and AC projections to project the REC.

2.2. Training the temperature sensitivity model for the French REC

To apply the temperature sensitivity model to the case of France at the finest spatial scales, one needs (i) pairs of input and target historical data to train and validate the model and (ii) input data from 21st century temperature projections on which to apply the trained model to project the REC. We present the training and validation data set in this subsection while the presentation of the 21st century temperature projections is left for Section 2.3.

We thus need data for the inputs of the model: the yearly DD, electric-heating rates, and AC adoption rates. The former is computed from daily surface air temperatures and heating and cooling setpoints. The target $E_i(y)$ is computed from the cell's REC and living surface. Several of these variables used to compute both the inputs and the targets are taken from a dataset provided by the French distribution system operator, Enedis. We first present this dataset and then describe how it is crossed with additional data sources to produce the input and the target training data. The longest training period that the following datasets permit ranges from 2011 to 2018 (included), which is the training period we use.

2.2.1. Energy and building characteristics per cell

The Enedis dataset is accessed via their website (Enedis, 2020) and includes the following variables that are relevant to this study:

- longitude and latitude coordinates of the cell centroids used to assign meteorological stations to cells in Section 2.2.2;
- yearly REC data per cell from 2011 to 2018 (included) used as the target in Section 2.2.5;
- electric-heating rates η_i^{El} for 2018;
- fraction of cell buildings with surfaces in different intervals used to compute the target in Section 2.2.5;
- Enedis estimates of β^{H} using a linear model based on DD akin to the model (2) (see below);
- yearly HDDs used in this Enedis model since 2018, but only at the department level, thus not satisfying our needs;
- heating setpoints used to estimate the HDDs used here as described Section 2.2.3;

Table 2
Heating setpoints T_r^H for all regions of metropolitan France computed according to Section 2.2.3.

Region name	T_r^H [°C]
Auvergne-Rhône-Alpes	16.0
Bourgogne-Franche-Comté	16.3
Brittany	14.8
Centre-Val-Loire	15.0
Grand-Est	16.6
Hauts-de-France	16.0
Ile-de-France	15.8
Normandie	15.0
Nouvelle-Aquiaine	15.3
Occitanie	16.4
Provance-Alpes-Côte d'Azur (PACA)	17.4
Pays-de-la-Loire	15.0

Table 3
AC adoption rates (%) for 2011 and 2018.

Region name	η^{AC}_{2011}	η^{AC}_{2018}
Auvergne-Rhône-Alpes	4.3	17.4
Bourgogne-Franche-Comté	3.4	13.9
Brittany	2.5	10.5
Centre-Val-Loire	4.0	16.5
Grand-Est	3.4	13.9
Hauts-de-France	2.5	10.5
Ile-de-France	4.5	18.3
Normandie	2.7	11.3
Nouvelle-Aquiaine	4.3	17.4
Occitanie	5.6	22.6
PACA	10.5	41.7
Pays-de-la-Loire	2.9	12.2

The Enedis estimates of β^{H} rely on consumption data at higher temporal resolutions (semi-annual, monthly, or daily) than the publicly available data. They thus can fit their temperature sensitivity model at the highest temporal resolution and average over each cell the estimated β^{H} for the different delivery points in the cell. However, the β^{H} of a cell is provided only if the estimate is considered sufficiently precise, i.e. if a minimum of 500 delivery points is available in the cell. As a result, around 50% of the cells are missing, whereas the model (2) can be applied to the annual consumption data to provide estimates of the temperature sensitivities for all cells in France.

2.2.2. Surface temperatures for training

To train the model (2), we use E-OBS version 20.0 (ECA&D, 2020) of the European Climate Assessment & Data (Klok and Klein Tank, 2009; Cornes et al., 2018) (ECA&D for continental gridded surface air temperature (Haylock et al., 2008). This gridded dataset is available at daily timesteps and a spatial resolution of 0.1 ° over Europe and the Mediterranean and spans from 1950 to the present. Among the available daily statistics, only the daily mean is retained here. Data observations are aggregated from several weather stations and gridded using an interpolation procedure combining spline interpolation and kriging. This dataset is a reference dataset for regional climate studies [e.g. (Haylock and Goodess, 2004; Santos et al., 2007; Stefanon et al., 2012; Raymond et al., 2016; Raymond et al., 2018)] and the evaluation of regional climate models [e.g. (Frei et al., 2003; Räisänen et al., 2004; Kjellström et al., 2010; Flaounas et al., 2013; Stéfanon et al., 2014; Ayar et al., 2016; Drobinski et al., 2018; Raymond et al., 2018)]. E-OBS includes some errors and uncertainties (changes in station locations or can induce those interpolation uncertainties, for example). Flaounas et al. (2013) assessed the E-OBS gridded dataset with temperatures displaying relatively small biases.

The temperature sensitivity model (2) requires temperatures for each cell to compute the HDD and CDD, but the cells (i.e. the IRIS in the case of France) do not correspond to the E-OBS grid points. We thus need to adjust E-OBS gridded temperatures to the cells over the French domain. This is done here using a nearest-neighbor interpolation using the Euclidean distance between temperature grid points and the cell centroids from Enedis (Section 2.2.1) in a plate carrée projected coordinate system. In order to match the target REC data from Enedis (Section 2.2.1), only the E-OBS data is kept from 2011 to 2018 (included) is kept as training input.

2.2.3. Heating and cooling setpoints estimates

A couple of temperature setpoints T_i^H and T_i^C are required for each cell i in order to compute the HDDs and the CDDs in the temperature sensitivity model (2). The estimation of the temperature setpoints is based on those available in the Enedis dataset (Section 2.2.1) and which Enedis uses to compute the HDDs in their own temperature sensitivity model. In our case, the model is simplified by identifying T_i^H for each cell i in the given administrative region r of France with the average T_r^H of all the values of T^H provided by Enedis for locations in r. The heating setpoint is thus constant over each region, i.e. $T_i^H = T_r^H$ for all cells i in r, where r runs over all the administrative regions of France. The resulting T_r^H estimates are shown in Table 2.

On the other hand, no cooling setpoints are provided by Enedis. Instead, we fix T_i^C for all the cells in France to the value of 21 °C used by EUROSTAT (YYYY) and International Energy Agency (2020).

Another approach to choose T_i^H and T_i^C could be to assume that these temperature setpoints are constant inside each region and to fit them as hyperparameters via a grid search. Doing so, it is found that the prediction error estimated via cross-validation is only marginally improved and that the main conclusions of this study remain unchanged (not shown here). Considering the higher complexity of this approach, the methodology presented in the previous paragraphs of this subsection is preferred here.

2.2.4. AC adoption rates for training

In addition to surface temperatures, the model (2) requires as input AC adoption rates η_i^{AC} for each cell in France. However, this information is not available at such a small geographical scale. Based on the evolution of the national AC adoption rate (ADEME, CODA STRATEGIES, 2021) and the regional distribution data in 2019 (Daguenet et al., 2021), we estimated the regional AC adoption rates at the regional level between 2011 and 2020 and assumed that all cells inside one administration region share the same adoption rate, i.e. $\eta_i^{\mathrm{AC}}(y) = \eta_r^{\mathrm{AC}}(y)$. This progression in AC adoption rate during the training period is assumed to be geometric. We calculated the average ratio between different years, which indicates a growth of 20% between two consecutive years. This AC adoption rate progression ratio is assumed constant during training, i.e. $\frac{\eta_i^{\mathrm{AC}}(y+1)}{\eta_i^{\mathrm{AC}}(y)} = \text{constant} = 120\%$. The population-weighted national average is then compared to the reference used in ADEME, CODA STRATEGIES (2021) and is consistent for 2016–2020. The estimated rate for the years 2011 and 2018 are shown in Table 3 with in between a geometric evolution. More details about the initial data used for the estimation can be found in Section C. Errors due to this factor are not studied but should be kept in mind as a limit due to the accessibility of data.

2.2.5. Living area to standardize REC

The model (2) is trained using as targets the yearly REC data from the Enedis dataset (Section 2.2.1). See in Section A for the details of the REC dataset. However, we are interested in the consumption per unit of area. Moreover, the number of buildings per cell — also provided by Enedis — varies from one year to the next. We thus need to normalize the REC of each cell by the corresponding total living surface. Unfortunately, Enedis does not provide the total living surface but the fraction τ_i^k of buildings in cell i for which the living surface belongs to an interval I_k in $\{(0,30),(30,40),(40,60),(60,80),(80,100),(100,+\infty)\}$ (m^2). Owing

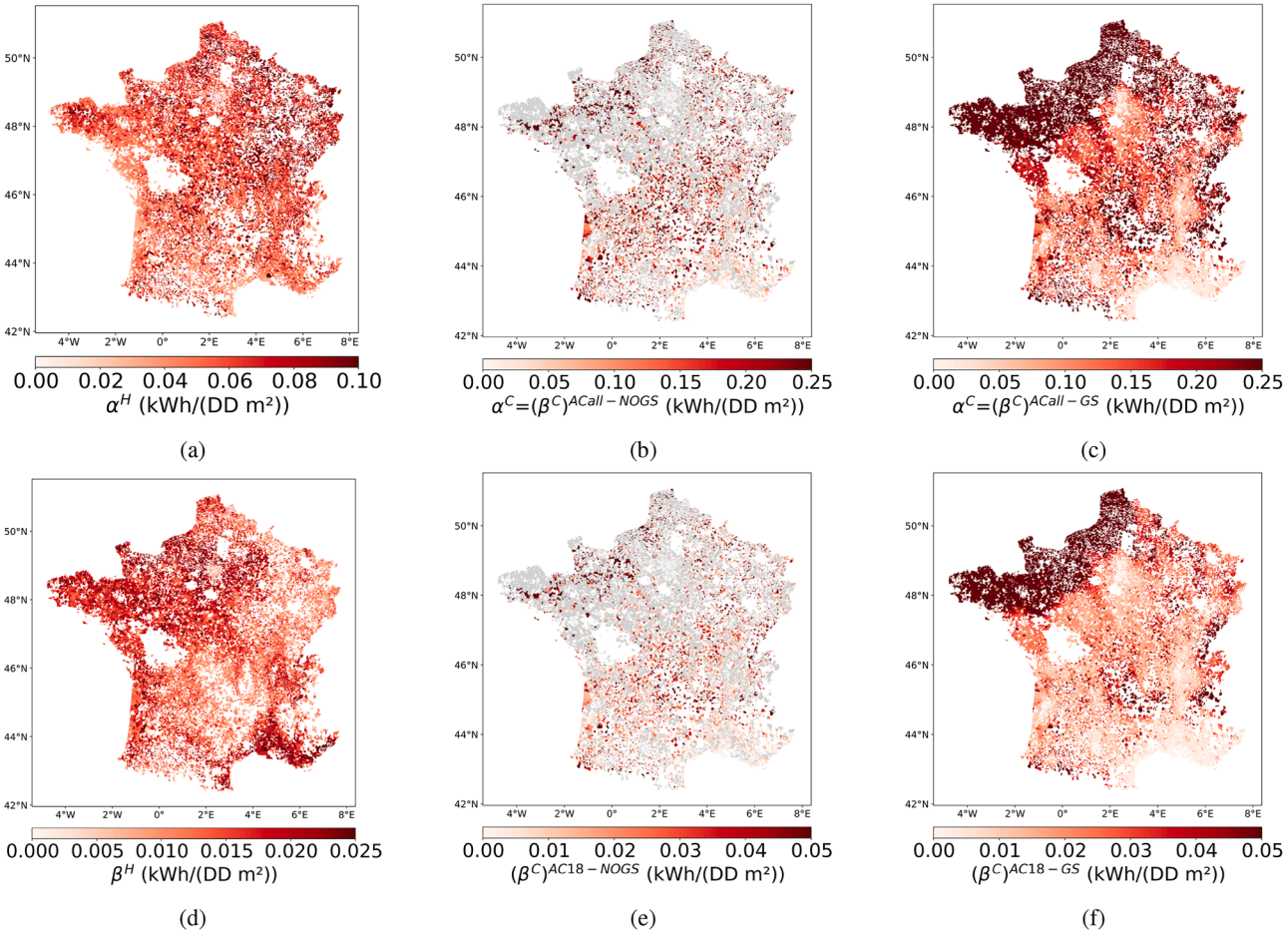

Fig. 3. Top: Estimates of α^{H} (left) and α^{C} (middle) obtained by training the model (2) on the observational data (Section 2.2). Projections of α^{C} (right) by gradual spreading (Section 2.3.2). Bottom: Corresponding values of β^{H} (left) and β^{C} (middle), and projections of β^{C} (right) for the AC2018 scenario (Section 2.3.2).

to the data constraints, we cannot get more specific information at the building level and can only present the distribution of intervals at the IRIS level. Thus, for each interval, we approximate the living surface of buildings with a surface in I_k by the center C_k (m^2) of the interval, except for the first and last intervals. We take the end value of 30 m^2 for the first interval rather than the median value due to the legal limitations on small living surfaces. For the last interval, we take the finite end of the interval 100 m^2, primarily because we lack further information on the distribution within the interval and also to counterbalance any potential overestimation for the first interval. It's important to note that these assumptions were made out of necessity due to the data limitations, and the accuracy of these estimates could potentially be improved with data availability at the building level. Then, the average living surface is estimated from the τ_i^k provided by Enedis with the following formula:

$$\overline{S}_i = \sum_k \tau_i^k C_k \quad \left(\mathrm{m}^2\right). \tag{3}$$

2.2.6. Trained temperature sensitivities

As an intermediate methodological result, the maps of the estimated α^{H} and α^{C} and corresponding β^{H} and β^{C} for cells with statistically significant coefficients at the 5% significance level (60% of all cells) are shown in the left and middle panels of Fig. 3. The OLS regression was used with a constraint on coefficients to be positive. Regression methods with regularization (Lasso and Ridge) were also tested, but this led to an increase in the test R^2 score of less than 10% (not shown here), so the OLS was preferred to limit the number of parameters of the model. All the test scores are estimated using k-fold cross-validation with one fold per year of data (8 folds in total). The test R^2 score averaged over all cells is about 0.68 with a 25% quartile of 0.56 and a 75% quartile of 0.79. More details about the test R^2 score are given in Section B as well as the validation of the model with comparison to Enedis datasets in Section A.

2.3. Projection data and scenarios definitions

As mentioned in Section 2.1, the basic consumption, represented by B in (2), is assumed to be stationary all the time. As far as the heating REC is concerned, we assume that α^{H}, T^H and η^{El} are also stationary so that only the HDDs change in response to temperature changes. Regarding the cooling REC, we follow a similar approach as for the heating REC, but η^{AC} and α^{C} also change in some AC scenarios (T^C is always stationary). We thus need to associate each cell with a temperature projection for a given climate change pathway, as well as with projections of η^{AC} and of α^{C}.

2.3.1. Temperature projection data under a climate change pathway

In this study, the most severe climate change pathway, the Representative Concentration Pathways (RCP) 8.5, is selected. The corresponding bias-corrected daily-mean temperature change is obtained from multiple regional climate models from the CORDEX program. In this study, these projections are completed with the corresponding historical experiments that serve as a reference to measure the effect of climate change. Due to modeling uncertainty, the projected statistics of the atmosphere may vary significantly with the choice of Regional Climate Model (RCM) and of driving Global Climate Model (GCM). Hence, multi-model ensembles are commonly used in climate studies to

Table 4
Institute, GCM name and RCP name for the 5 climate change simulations used in this study.

No.	Institute	Driving GCM model	RCM model
1	CNRM	CERFACS-CM5	ARPEGE51
2	CNRM	CERFACS-CM5	RCA4
3	IPSL	CM5A-MR	RCA4
4	IPSL	CM5A-MR	WRF331F
5	ICHEC	EC-EARTH	RACM022E

provide a partial estimation of the modeling error. This is why the five model combinations listed in Table 4 are used in this study. These simulations are accessed via the Copernicus Climate Change Service database (https://climate.copernicus.eu/).

To associate a cell to a climate-model simulation, the same methodology as for the temperature observations used for training is followed (Section 2.2.2). Three climate-simulation periods of 30 years are considered, which are distinct from the training period defined in Section 2.2: a historical period from 1975 to 2005 (excluded) — used as reference — and two projection periods, one from 2025 to 2055 and one from 2070 to 2100. Results associated with the latter are respectively referred to as CC2040 and CC2085 (based on the central year of the period).

As intermediate methodological results, mean historical HDD and CDDs, as well as the corresponding projected changes, are represented in Fig. 4. One can see that the temperature increase projected over France leads to a general decrease in the HDDs (top panels) and to a general increase in the CDDs. These changes are however not homogeneous since the decrease in the HDDs is strongest in the southern and eastern parts of France, while the increase in the CDDs is largest in the southern part of France.

2.3.2. AC use scenarios

In the present framework, two factors are sensitive to the evolution of AC use during the 21st century: the AC adoption rate η_i^{AC}, and the switch of a cell from an α_i^C of zero to a positive α_i^C, for each cell i. While the former reflects the evolution of AC use within a cell, the latter corresponds to a conversion of a cell from having no AC user at all to having some AC users. Here, we do not attempt to make plausible projections of these factors based on current signals. Instead, as summarized in Table 5

Table 5
Definition of the four AC scenarios in terms of AC adoption rate and α^C spreading strategy. XXXX is either 2040 or 2085, corresponding to the central year of the climate change projection window considered.

Name	Definition	
	η^{AC}	Gradual Spreading of α^C
CCXXXX-AC18-NOGS	Same as in 2018	No
CCXXXX-AC18-GS	Same as in 2018	Yes
CCXXXX-ACall-NOGS	100%	No
CCXXXX-ACall-GS	100%	Yes

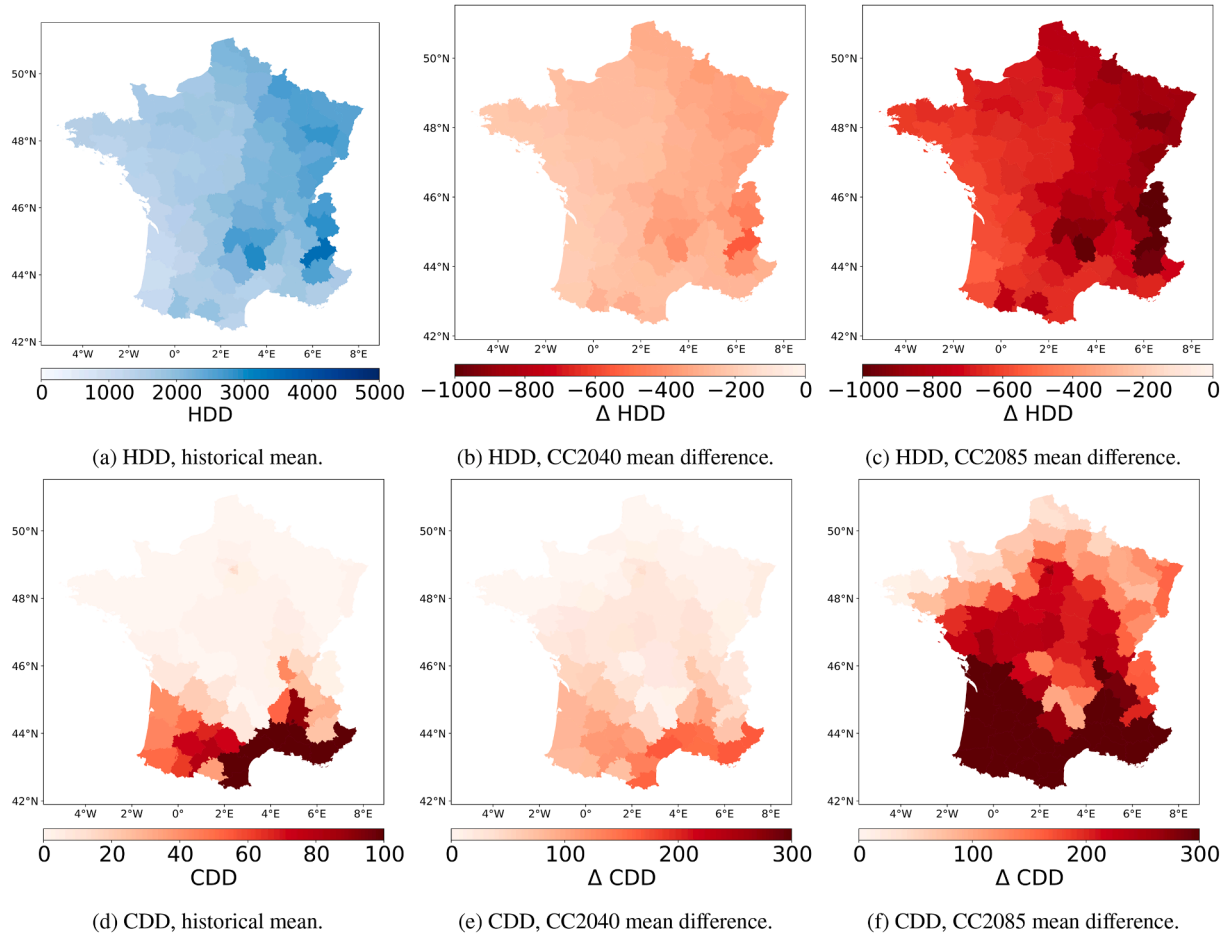

(a) HDD, historical mean. (b) HDD, CC2040 mean difference. (c) HDD, CC2085 mean difference.

(d) CDD, historical mean. (e) CDD, CC2040 mean difference. (f) CDD, CC2085 mean difference.

Fig. 4. Mean over 1975–2005, mean change over 2025–2055 wrt. 1975–2005 (CC2040), and mean change over 2070–2100 wrt. 1975–2005 (CC2085) for the HDDs (top) and CDDs (bottom) computed according to Eq. 1. The temperature data for 1975–2005 is from the historical CORDEX simulations, while that for 2025–2055 and 2070–2100 is from the RCP8.5 CORDEX simulations. The results are spatially averaged over the departments and averaged over the climate-model simulations listed in Table 4. Warm colors represent situations associated with warm temperatures (i.e. to a decrease in heating REC and to an increase in cooling REC).

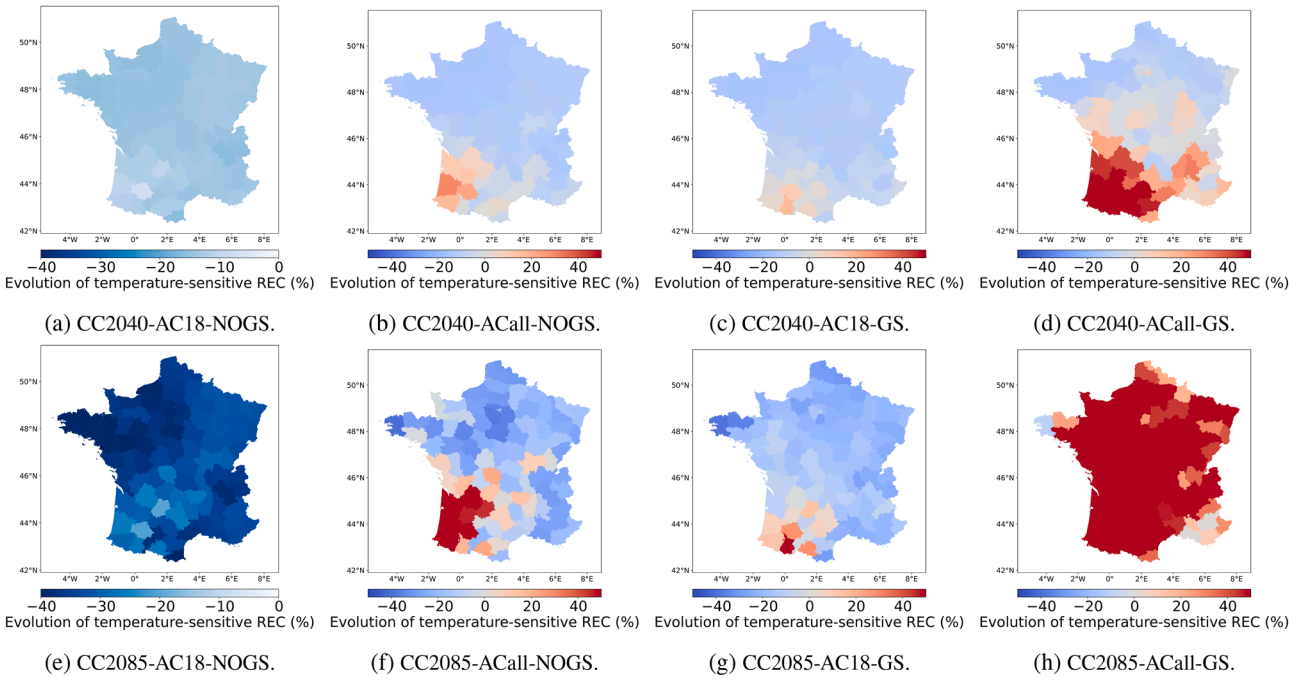

(a) CC2040-AC18-NOGS. (b) CC2040-ACall-NOGS. (c) CC2040-AC18-GS. (d) CC2040-ACall-GS.

(e) CC2085-AC18-NOGS. (f) CC2085-ACall-NOGS. (g) CC2085-AC18-GS. (h) CC2085-ACall-GS.

Fig. 5. Relative change (%) in REC wrt. to the historical period (1975–2005) for CC2040 (top) and CC2085 (bottom) and for different AC scenarios: AC18-NOGS (left column), ACall-NOGS (second column), AC18-GS (third column) and ACall-GS (right column).

and explained below, two extreme cases are considered for both factors and indifferently for the 2025–2055 and the 2070–2100 periods.

Regarding η^{AC}, the minimal scenario is that η^{AC} remains fixed to its 2018 cell values (Section 2.2.4), corresponding to a situation in which AC installation no longer progresses. The maximal scenario is that η^{AC} has reached 100% in every cell before the beginning of the projection period and remains fixed over the period, corresponding to a situation in which all households are equipped with AC (regardless of the technology).

Regarding α^{C}, the minimal scenario is that cells with no cooling temperature sensitivity remain so. The maximal scenario is that all cells become cooling-sensitive. In this case, further assumptions are needed to determine α^{C} for these cells that were not cooling-sensitive historically. Here, we assume that α^{C} for these cells is the result of interpolation from the α^{C} values of the surrounding cells with a positive α^{C}. A nearest-neighbor interpolation is performed for a given number of neighbors and for the Euclidean distance in the plate carrée projection. The number of neighbors is optimized based on the methodology described in Section D, giving an optimal number of 25 cells. We refer to this scenario as the gradual spreading of α^{C} and the resulting α^{C} estimates are shown in Fig. 3c. The gradual spreading scenario mimics a "do like my neighbor" behavior.

2.4. Quantifying the uncertainty in the projected REC change

For a given cell i, a model m (Table 4 and a scenario s (Table 5), we define the absolute change in REC, $\Delta\overline{E}_i^{m,s}$, as the difference ($\Delta$) at i between the REC averaged ($\bar{\cdot}$) over the CORDEX historical period and the REC averaged over one of the two CORDEX projection periods, estimated with the model m simulations for the scenario s. In addition, the relative REC change is defined as the absolute REC change divided by the REC averaged over the CORDEX historical period. Given the stationarity assumptions (Section 2.3), the absolute REC change is given by

$$\Delta\overline{E}_i^{m,s} = \alpha_i^{\mathrm{H}}\eta_i^{\mathrm{El}}\Delta[\overline{\mathrm{HDD}}_i^{m,s}] + \Delta\left[\left(\alpha_i^{\mathrm{C}}\eta_i^{\mathrm{AC}}\right)^{s}\overline{\mathrm{CDD}}_i^{m,s}\right]. \tag{4}$$

In the AC18-NOGS scenario, α^{C} and η^{AC} are also stationary, so that

$$\Delta\overline{E}_i^{m,s} = \alpha_i^{\mathrm{H}}\eta_i^{\mathrm{El}}\Delta[\overline{\mathrm{HDD}}_i^{m,s}] + \left(\alpha_i^{\mathrm{C}}\eta_i^{\mathrm{AC}}\right)^{\mathrm{AC18-NOGS}}\Delta[\overline{\mathrm{CDD}}_i^{m,s}], \tag{5}$$

in this case.

The corresponding multi-model average is

$$\left\langle \Delta\overline{E}_i^{s} \right\rangle := \frac{1}{M}\sum_{m=0}^{M-1}\Delta\overline{E}_i^{m,s}. \tag{6}$$

An essential part of this study is quantifying the uncertainty of our estimates of temperature-sensitive REC change $\langle\Delta\overline{E}_i^{s}\rangle$. From (6), we can see that errors may come from.

- the temperature sensitivity model design,
- the stationarity assumptions on the model coefficients and on electric appliances adoption rate η_i^{El} and η_i^{AC} during scenarios studies,
- the regression of the coefficients from a particular training dataset,
- the historical estimates of η_i^{El} and η_i^{AC},
- the climate models (Jacob et al., 2014; Ruti et al., 2016),
- the choice of climate change pathway and AC use scenario.

Here, only the worst-case climate change pathway is considered (i.e. RCP8.5, Section 2.3.1), so that uncertainty in the climate-model pathway is not assessed. On the other hand, a partial estimate of climate-model errors is provided in the results Section 3 from the variations of the projected REC change with the choice of the climate model. To estimate the sensitivity of temperature-sensitive REC change to AC adoption rate projections, extreme scenarios are considered (Section 2.3), while measurements of the electric-heating rate are assumed to be reliable and representative of other years than the year it is provided for. The assumption of the stationary temperature sensitivity model coefficients restricts the scope of the results of this study. It is not tested in-depth in this work, but a simple analysis is conducted in Section 3.2 and further discussed in terms of policy implications in Section 4. Finally, the errors from the model design and the regression are estimated using cross-validation (Section 3.4).

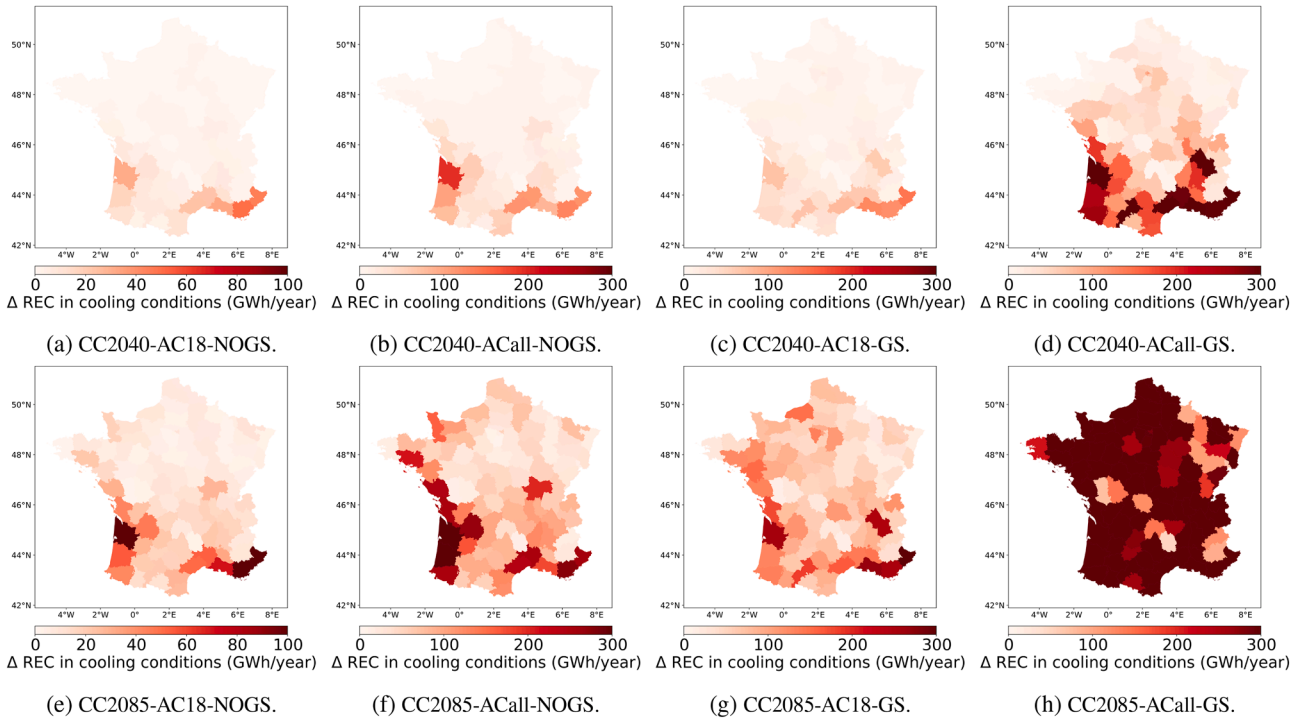

Fig. 7. Same as Fig. 5 but for th.e cooling REC.

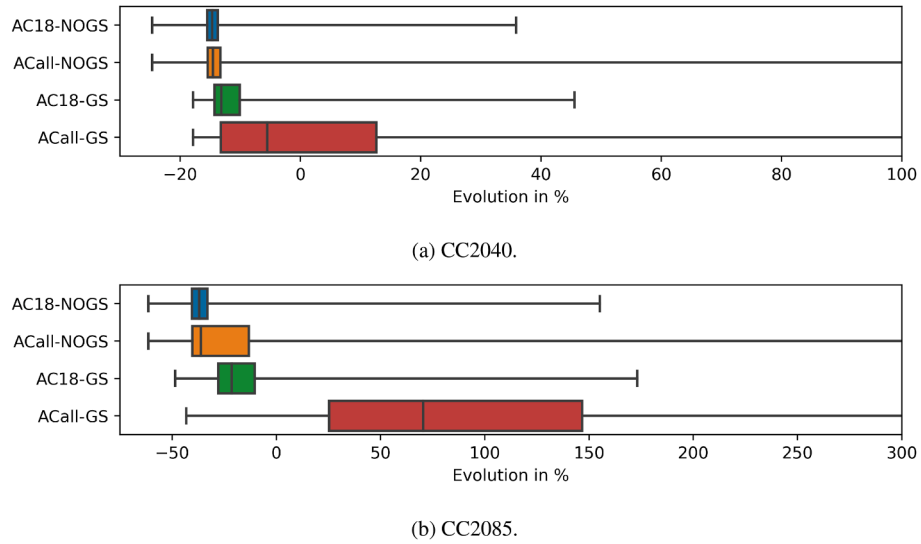

Fig. 6. Boxplots over the cells of the relative change in temperature-sensitive REC corresponding to Fig. 5. The whiskers here show the minimum on the left and the 99% quantile on the right.

Table 6
Decomposition of variability into different geographical scales for different studied variables in terms of proportion (%).

Variable y_i	$\frac{\sigma^2(y_i - \langle y_i\rangle_d)}{\sigma^2(y_i)}$	$\frac{\sigma^2(\langle y_i\rangle_d - \langle y_i\rangle_r)}{\sigma^2(y_i)}$	$\frac{\sigma^2(\langle y_i\rangle_r - \langle y_i\rangle_n)}{\sigma^2(y_i)}$
β_i^{H}	75%	13%	12%
α_i^{C}	77%	4%	19%
$\langle \Delta\overline{\mathrm{HDD}}_i \rangle^{\mathrm{CC2040}}$	24%	20%	56%
$\langle \Delta\overline{\mathrm{HDD}}_i \rangle^{\mathrm{CC2085}}$	29%	23%	48%
$\langle \Delta\overline{\mathrm{CDD}}_i \rangle^{\mathrm{CC2040}}$	13%	15%	72%
$\langle \Delta\overline{\mathrm{CDD}}_i \rangle^{\mathrm{CC2085}}$	14%	13%	73%
$\langle \Delta\overline{E}_i \rangle^{\mathrm{AC18-NOGS}}$	82%	7%	11%

3. Results and discussion

We now analyze the projected changes in the REC, first for the scenarios where the AC uses remain fixed, then for scenarios with AC uses changes. The discussion of the uncertainty in the results is left for the next Section 4, the main conclusions from these results being robust.

3.1. Projected REC change without change in AC use

The projections of temperature-sensitive REC changes for fixed AC use (AC18-NOGS) are shown in Fig. 5a and Fig. 5e. In general, the REC decreases between 7% and 16% in all departments for CC2040, down to 20% to 42% for CC2085. Aggregated at the country scale, the REC

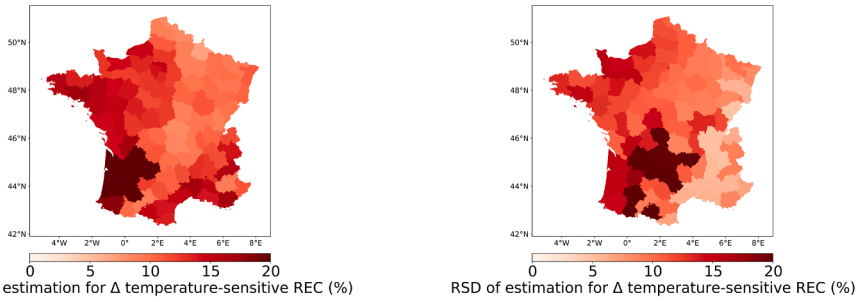

(a) CC2040-AC18-NOGS. (b) CC2085-AC18-NOGS.

Fig. 8. The global uncertainty of estimation of evolution in temperature-sensitive REC by combining all possible estimated coefficients with the leave-one-out cross-validation method and the 5 CORDEX simulations, represented by the Relative Standard Deviation (RSD) for the CC2040-AC18-NOGS (left) and the CC2085-AC18-NOGS (right) scenarios.

Table 7
Average values with uncertainty for all possible combinations, the uncertainty is converted to the same magnitude by averaging over the number of cells. A t-test shows that mean values of REC change under all scenarios are significant.

Time	Scenario name	Mean (GWh/cell)	Std (GWh/cell)		
			Cell	Department	Country
2040	CC-AC18-NOGS	−0.22	0.037	0.029	0.024
	CC-AC18-GS	−0.16	0.053	0.038	0.031
	CC-ACall-NOGS	−0.16	0.066	0.042	0.032
	CC-ACall-GS	0.08	0.191	0.146	0.125
2085	CC-AC18-NOGS	−0.53	0.085	0.057	0.047
	CC-AC18-GS	−0.28	0.185	0.150	0.136
	CC-ACall-NOGS	−0.26	0.236	0.159	0.138
	CC-ACall-GS	1.26	1.019	0.867	0.790

Table 8
Comparison of uncertainty due to model or CORDEX for scenario AC18-NOGS in the form of standard deviation (GWh/cell).

Time	Cell		Commune		Country	
	Model	CORDEX	Model	CORDEX	Model	CORDEX
2040	0.020	0.034	0.012	0.029	0.010	0.022
2085	0.056	0.066	0.031	0.052	0.026	0.040

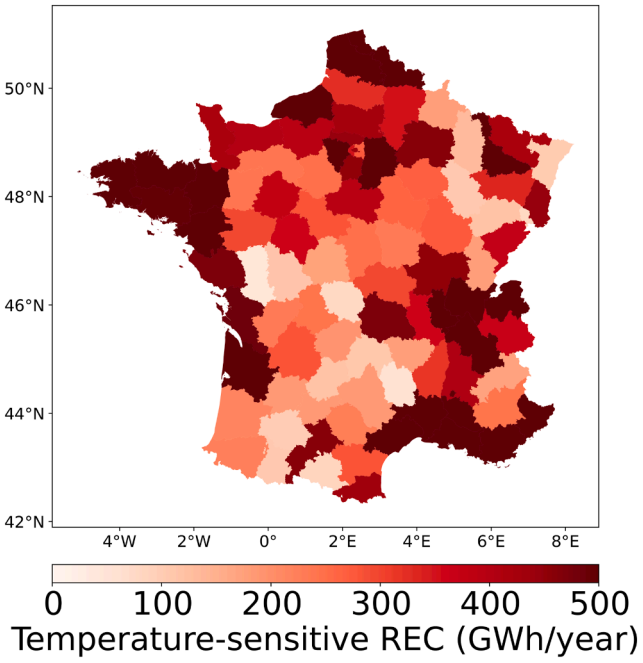

Fig. 10. Total temperature-sensitive REC reference aggregated at the department level, estimated with our model using the temperature of 1975–2005 from CORDEX simulations on all valid cells (60% of the cells).

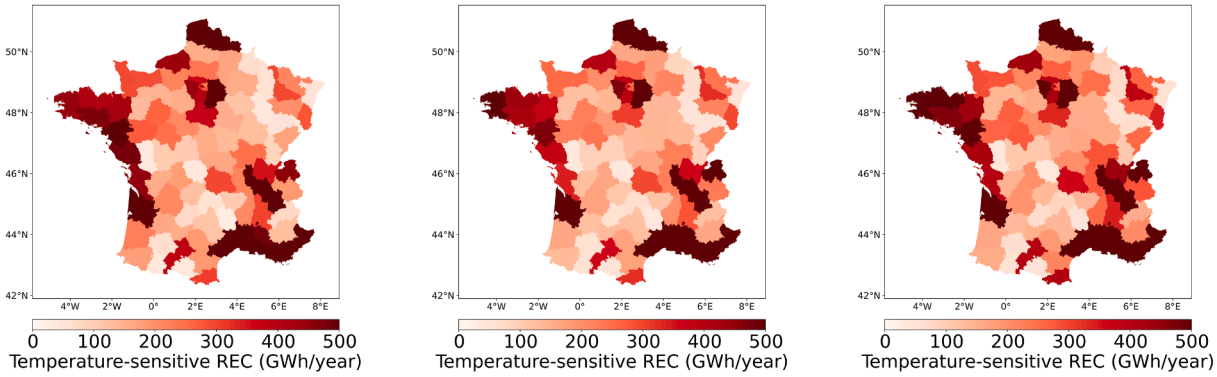

(a) (b) (c)

Fig. 9. Temperature-sensitive REC per year averaged over departments estimated from (a) the Enedis ρ^{H} estimates for 2018 (for 50% of the cells only, Section 2.2.1), (b the model (2) applied to the E-OBS temperatures for 2018 and (c) the model (2) applied to the CORDEX historical temperatures over the 1975–2005 period and averaged over the period and over the climate-model simulations (Section 2.3.1).

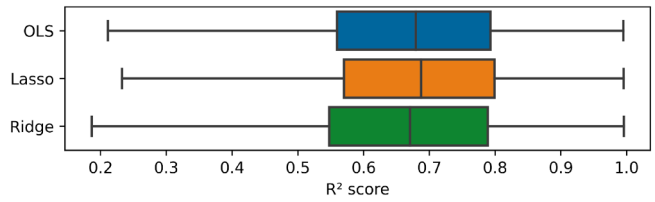

Fig. 11. Comparison between linear regression methods of R^2 score distribution for all valid IRIS.

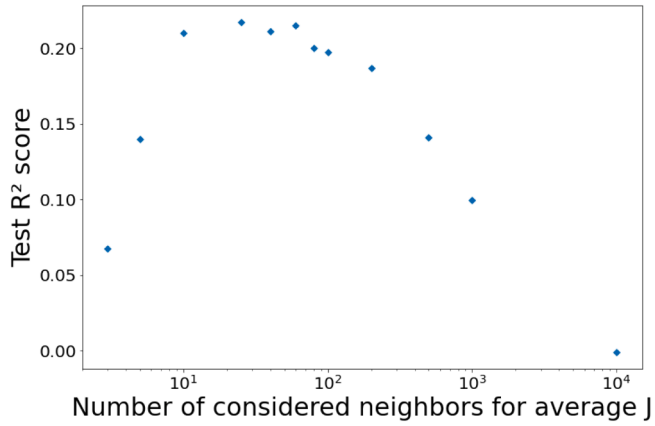

Fig. 12. Test R^2 score between estimated α_i^C with Gradual Spreading method and regression model estimation as a function of the chosen number of neighbors J taken into account for the calculation of average (Gradual Spreading).

decreases by about 8TWh and 20TWh, respectively. This is consistent with the results of Damm et al. (2017); Spinoni et al., 2018, but significant variations are observed between departments.

For this scenario and for a given cell, according to (5), the projected heating and cooling REC changes are proportional to the HDD and CDD changes, respectively, represented in Fig. 4. However, the coefficients of proportionality, $\alpha_i^H \eta_i^{El}$ and $(\alpha_i^C \eta_i^{AC})^{AC18-NOGS}$, represented in Fig. 3, depend on the cell. From this can be deduced that the REC changes for this scenario are dominated by the large decrease in the HDDs (Fig. 4b and Fig. 4c) modulated by variations in β^H with the cells (Fig. 3d). This effect can for instance be seen in the weaker reduction of the REC in the North-East and the South-West of France.

In addition, the REC decrease is reduced in the south of France due to the significant increase in the cooling REC with the increase in the CDDs (Fig. 4e and Fig. 4f) in conjunction with the positive β^C there (Fig. 3e). This is more obvious from the plots of the cooling REC for the AC18-NOGS scenario in Fig. 7a and Fig. 7e. One can see that, according to this scenario, the cooling REC increases everywhere, but this is particularly evident along the Atlantic coast and South of 46 °N latitude, between the Massif Central and the Alps, especially for the CC2085 period. At these locations, HDDs indeed tend to increase significantly, but the correlation is not perfect, since, for this scenario, the translation of this change in a cooling REC change depends on AC being already in use there (Fig. 3e). A substantial increase in the cooling REC is also observed in the Northwest part of France for CC2085 (Fig. 7f), even though the increase in CDDs is relatively weak there (Fig. 4f). This is explained by the fact that a significant number of cells there have a large β^C (Fig. 3e).

The distribution of the temperature-sensitive REC change at the cell level is shown in Fig. 6 in the form of box plots. The distribution for scenario CC2040 without AC use changes (AC18-NOGS) is right-skewed, meaning the temperature-sensitive REC is expected to decrease around 15% in most regions. In the longer term, the disparity between IRIS increases with decreasing averaged temperature-sensitive REC. Indeed, some IRIS may display a positive temperature-sensitive REC change (i.e. an increase in temperature-sensitive REC) over 3% of the French territory in the near future and up to 7% by the end of the 21st century.

3.2. Projected REC change with change in AC use

The projections of temperature-sensitive REC change with different AC scenarios are shown in 5b-5d and 5f-5h. Contrary to the results including temperature change only, some regions display an increase of temperature-sensitive REC whose pace and spatial extent depend on the AC scenario.

Results also show that the different factors have diverse effects. In the case where the AC rate is changed without spreading geographically, the temperature-sensitive REC is expected to increase in the South-West of France and in the South along the Mediterranean Sea (Fig. 5b and Fig. 5f). Indeed, in this region, α^H is relatively low with respect to other regions, and AC systems are already deployed so that α^C is different from zero. But α^C in these regions has a relatively low value, so if the temperature change is only accounted for, increased CDD makes the decline in temperature-sensitive REC less rapid. However, in the considered scenario, the change in AC rate directly multiplies the current cooling demand by four to five times. The electricity savings from heating in the South-West are thus expected to be fully offset by cooling in the near future (Fig. 7b). In the far future, this trend should be exacerbated in the South-West and in the South and spread significantly along the Atlantic coast and South of 46 °N (Fig. 7f). As there is no spatial spreading of AC usage, the geographical patterns of temperature-sensitive REC change are similar between Fig. 7a and Fig. 7e, and Fig. 7b and Fig. 7f.

With regards to the AC rate scenario, the gradual spreading of the present AC rate lowers the change of REC for cooling needs, but REC for cooling needs becoming positive spreads geographically (Fig. 5c and Fig. 5g). Gradual spreading does not change the values instantly in regions where most IRIS cells are already given with non-null estimation for α^C. However, it helps to smooth the map of coefficients as shown in Fig. 3b and Fig. 3c. Based on observational data, many cells in Ile-de-France, Auvergne-Rhône-Alpes, and along the Atlantic coast have been given null estimates for α^C. However, some nearby cells still received significant values for α^C with high regression scores. Assigned with proximity averages, these areas mixed with sporadic large values are most affected. Fig. 6 shows that a 100% AC rate in already equipped cells (ACall-NOGS) modifies the shape of the distribution, with an increased number of cells with positive evolution. More positive values correspond to the cells currently equipped with AC at which the AC rate is increased from its current value to 100% and where the change of REC for cooling needs exceeds that for heating needs. No change is expected for the cells currently without AC hence the minimal, the first quartile even the median values remain the same as for AC18-NOGS. In the gradual spreading scenario (AC18-GS), the shape of the distribution displays an even larger positive skewness than in the 100% AC rate scenario. Less negative values correspond to the larger number of cells equipped with AC and bring an increase to all cells.

In a scenario combining gradual spreading and 100% AC rate, almost half of the territory, except the North of France, sees the REC increasing in the near-term future, amounting to a global change of +2%. At the end of the 21st century, this fraction of positive trend increases up to 90%, leading to a global change of +32%.

The results of these scenarios motivate actions allowing at least to prevent AC from inducing an increase in cooling REC. A simple approach, applicable to the whole country, consists at least in the region of South of France with the greatest AC impact to modify in the future climate scenarios only the cooling setpoint in such a way as to maintain the cooling REC unchanged with respect to the present situation. Such an approach leads to the most constraining action as it sets for the whole country the highest cooling setpoint, but it ensures at least unchanged cooling REC in the South of France and in most regions of France a

negative cooling REC trend. The cooling setpoint preventing any cooling REC increase over the whole country varies with the time horizon, which is about 23–24 °C by 2040 and 26–27 °C by 2085.

3.3. Spatial heterogeneity

The maps shown in Fig. 3 and Fig. 5 show an apparent geographical disparity of temperature sensitivities and temperature-sensitive REC changes. To compare the intra-department variability with the one of inter-department, each studied variable y_i (sensitivity coefficients α_i^H, α_i^C, DD evolution $\langle \Delta\overline{HDD}_i^s \rangle, \langle \Delta\overline{CDD}_i^s \rangle$ and the REC evolution $\langle \Delta\overline{E}_i^s \rangle$) can be decomposed as:

$$y_i = (y_i - \langle y_i \rangle_d) + (\langle y_i \rangle_d - \langle y_i \rangle_r) + (\langle y_i \rangle_r - \langle y_i \rangle_n) + \langle y_i \rangle_n. \quad (7)$$

with $\langle y_i \rangle_d$ the average value of cells inside a given department, $\langle y_i \rangle_r$ the average value of cells inside a given administrative region, and $\langle y_i \rangle_n$ the average value of all cells in France. Hence with the above equation, the variability of all cells can be decomposed into disparities at several stages:

$$\sigma^2(y_i) = \sigma^2(y_i - \langle y_i \rangle_d) + \sigma^2(\langle y_i \rangle_d - \langle y_i \rangle_r) + \sigma^2(\langle y_i \rangle_r - \langle y_i \rangle_n). \quad (8)$$

where $\sigma^2(y_i - \langle y_i \rangle_d)$ represents the variability of cells inside the department while $\sigma^2(\langle y_i \rangle_d - \langle y_i \rangle_r)$ represents the variability of departments inside a given administration region and $\sigma^2(\langle y_i \rangle_r - \langle y_i \rangle_n)$ the variability between different administrative regions. Table 6 shows the proportion of variability at each geographical scale over the whole variability.

The regional variability is more important than the local difference for the DD changes. However, the variability of temperature sensitivities between cells within the same department dominates. At the same time, because of the large spatial variability of β^H and α^C within the administrative regions, a larger disparity of temperature-sensitive REC changes is found between cells than between administrative regions. For both temperature sensitivities, β^H and α^C and temperature-sensitive REC changes, it shows that the variability between the cells is more significant than the difference between regions, which justifies our choice of study at a small geographical scale.

3.4. REC change error estimates

In this study, public data are used to train the temperature sensitivity model with only eight annual samples applied for the regression. Compared to models with a larger dataset, our model can be easily influenced by outliers and may have coefficients over-fitted.

We did not choose regularized regression because the performance did not improve much, but this method may be more attractive if a more extensive input is available. Nonetheless, the possibility of applying the leave-one-out cross-validation over the training gives us eight possible models and, thus, a range of eight different results of the temperature sensitivities with uncertainty.

At the same time, CORDEX simulations from different models may produce different future temperature projections. Combining the five different simulations and all possible estimated coefficients with the leave-one-out cross-validation method, the global uncertainty of our results, quantified by the Relative Standard Deviation (RSD), is shown in Fig. 8. The relative error is large in the South-West, where $\alpha^C > 0$, due to the biased model regressions as the observed temperatures do not largely and frequently exceed the 21 °C cooling setpoint.

The global uncertainty for all the scenarios is presented in Table 7. The standard deviation is identified after aggregating REC at different levels. For the results to have the same order of magnitude and to be comparable, the REC change is normalized by the average number of IRIS in the desired geographical scale. The method using a REC linear model together with the CORDEX simulations derives robust estimates of future REC with an error of less than 18.4% without assumptions on AC uses. The uncertainty of scenario ACall-GS is the largest among all other scenarios because the results may become less precise with all the assumptions together. We can see clearly that with spatial aggregation, the error decreases because there can be compensation between IRIS within the large scales, and the variation becomes smaller. For the average values of all possible combinations, a t-test shows that the mean values of REC change under all scenarios are significant.

The global error of future REC mainly comes from the multi-model ensemble spread of the projected temperatures and the training bias and variance of the REC linear model. To find the standard deviation due to different sources, we use the average values of the cross-validated coefficients estimated by the model or the average of the five simulations of CORDEX, respectively. The uncertainty due to the simulations of CORDEX and to the model regression can be found in the following Table 8. With the previous tables, we can see clearly that the uncertainty due to the various simulations of CORDEX leads to a more significant error than the one from the regression. This 10% error due to the model is reassuring the basis of a temperature sensitivity model: the temperature sensitivity is quasi-constant under a stable climate. Nevertheless, this error can still be improved if more annual consumption data are available or daily consumption data can be accessible.

4. Conclusions and policy implications

A number of key messages can be drawn from the results of this study. First, REC varies significantly at very fine spatial scales, from the IRIS size (region of 2,000 inhabitants) to the administrative departments (96 departments on the European continent and 5 overseas) and regions (13 on the European continent and 5 overseas). Such variability had never been quantified and mapped due to a lack of suited methodology and limited available data at the finest scale (IRIS). Such variability which is the largest at the finest spatial scale calls for solutions and policies steered to the local specificities.

With increasing temperatures due to climate change, the heating needs decrease especially in the North-East which displays a continental climate with very hot summers and very cold winters (Köppen, 1936) and thus a strong sensitivity to any heating need reduction. Conversely, the South and Western regions along the Mediterranean Sea and the Atlantic Ocean, respectively, display a smaller trend in heating needs as they display a Mediterranean climate (hot, dry summers and cool, wet winters) and a maritime climate (cool summers and mild winters) (Köppen, 1936), respectively with warmer winters with regards to the North-East of France. At the end of the 21st century, in the worst-case climate scenario (RCP8.5), the spatial variability of the trend decreases as many regions are expected to experience temperatures much more rarely below their heating setpoint. There is a strong link between the heating needs and its evolution with that of REC.

However, the evolution of REC is modulated by the evolution of cooling needs and the deployment of AC systems to meet those needs. Our worst-case scenarios suppose either a 100% AC adoption rate in the IRIS already equipped at present, or a gradual spreading of AC systems, which mimics a "do like my neighbor" behavior. We also consider a combination of the two. In any scenario, the decrease in REC due to climate change could be totally offset in the South of France, which would then display an increase in REC. When the 2 AC scenarios are combined, an increase in REC could be seen over the whole country.

One key message deals with the overall uncertainty of our modeling setup. The uncertainty of our REC trends, including climate change impact and AC system deployment, is dominated by the spread between the climate simulations of our ensemble. The regression-based REC model does not add up much to the overall uncertainty. Such a result was not straightforward as the data available at the IRIS scale was at best limited in time, at worst available on an annual basis only, and sparse in some regions. The level of overall uncertainty therefore allows for drawing some recommendations in terms of practical applications and energy policies.

Takeaways for policy implications can be formulated from these results. In our scenario, AC gradual spreading mimics a "do like my neighbor" behavior. Our results show that such behavior has a major and detrimental impact on REC (more than 100% AC rate scenario). Such results call for targeted and local information actions where the risk of spreading is high (i.e. in areas where households are already equipped with AC systems) to limit the spreading or mitigate its effect with at least the most energy-efficient AC systems. A more straightforward result is that the South of France is where the REC trend is expected to occur first with possible impacts on the energy system. Therefore there is a need to target actions to prevent any further deployment of AC systems. Especially, the climate of the South of France is expected to become similar to the present climate of countries more to the South, such as Italy or Morocco (Hallegatte et al., 2007). In Morocco, there is no visible impact on REC of AC use (Bouramdane et al., 2021). In Italy, the signal on REC of the use of AC is very limited (Tantet et al., 2019) but locally the evolution of cooling needs can have a significant impact on REC (De Felice et al., 2013; Scapin et al., 2016). Therefore, analyzing the socio-economic drivers, and the energy policies of these countries and drawing inspiration from them to deploy actions adapted to the local specificities of some French regions should be considered. Our worst-case results clearly show the detrimental impact of the increase in AC rate and spreading. Increasing the cooling setpoint T^C (e.g. recommended temperature of 26 °C by the US Department of Energy) or maintaining an optimal difference with outdoor air temperature to about 7–8 °C to maximize the energy efficiency of the AC equipment, could lower the cooling REC. Based on our model, shifting the cooling setpoint from 21 °C at present to 23–24 °C by 2040 and 26–27 °C by 2085 would prevent any cooling REC increase in our worst-case scenarios. These values are consistent with existing recommendations. Low-tech alternative solutions also exist which are widely implemented in subtropical regions, and can be implemented in France to improve the thermal comfort of buildings and reduce the use of AC equipment and their impact on the environment, such as the reflective white coating on the buildings or roofs (Viguié et al., 2020; Rawat et al., 2022).

There are still several limits to this study. The temperature sensitivity results from a regression between REC and temperature, and the model implicitly integrates "human behaviors" related to other factors such as electricity costs and household revenue (Frederiks et al., 2015; Gertler et al., 1366). However, at this stage, no approach to segment the consumption data along multiple socio-economic dimensions (e.g. price, revenue) has been successful with the available data (e.g. time sampling and spatial granularity too coarse and aggregated) which would have been valuable to reduce global uncertainty. It could have been relevant to perform a sensitivity analysis on the temperature sensitivity through η^{El} to account for the further electrification of heating (e.g. fuel oil or gas to heat pumps) or trough α^C to account for improved efficiency of AC systems. Regarding α^C, regions of the North-West along the Atlantic coast where the AC rate is on average 14% (versus 22% at the national level in 2019) can display surprisingly large positive α^C values. The causes should be further explored, whether due to statistical processing or behavioral in origin (e.g. residents may be less adapted to extreme heat events and more likely to install AC equipment for use during such extreme events (He et al., 2022)). Finally, the study from Pagliarini et al. (2019) shows that in a warmer climate, the electricity increases faster than linearly because of the efficiency drop of air-cooled chillers at high temperatures. Such a phenomenon should also be considered in the future.

CRediT authorship contribution statement

Qiqi Tao: Conceptualization, Data curation, Formal analysis, Investigation, Methodology, Visualization, Writing - original draft, Writing - review & editing. **Marie Naveau:** Conceptualization, Data curation, Formal analysis, Investigation, Methodology. **Alexis Tantet:** Conceptualization, Supervision, Validation, Writing - review & editing. **Jordi Badosa:** Conceptualization, Data curation, Formal analysis, Validation, Writing - review & editing. **Philippe Drobinski:** Conceptualization, Formal analysis, Supervision, Validation, Writing - review & editing.

Data availability

Input data are all publicly available, produced data will be made available by request.

Declaration of Competing Interest

The authors declare that they have no known competing financial interests or personal relationships that could have appeared to influence the work reported in this paper.

Data availability

Data will be made available on request.

Acknowledgments

This work was carried out at the Energy4Climate Interdisciplinary Center (E4C) of IP Paris and Ecole des Ponts, supported by 3rd Programme d'Investissements d'Avenir [ANR-18-EUR-0006–02]. It was funded by nam'R company through a collaboration grant. The authors thank L.G. Giraudet and V. Viguié for fruitful discussions and comments. We acknowledge the E-OBS dataset from the EU-FP6 project UERRA (http://www.uerra.eu) and the data providers in the ECA&D project (https://www.ecad.eu)

Appendix A. Reference REC and verification of climate data on REC

Fig. 9 shows the temperature-sensitive REC aggregating over the 12 administrative regions the values at the IRIS where such estimate by Enedis exists from Enedis processing (a), by applying the model (2) to temperatures from E-OBS dataset (b) and historical CORDEX simulations (c). Visually, the three show a very similar pattern. Fig. 9a and Fig. 9b illustrate the quality of the model prediction and quantitatively a R^2 score of 0.77 is found between the common cells. Fig. 9c shows how historical climate simulations can satisfactorily reproduce the temperature-sensitive REC for climate projection studies which rely on the climate projections produced in a consistent way with the historical climate simulations. However, in Section 3, the temperature-sensitive REC based on the CORDEX regional climate simulations is estimated over a larger number of IRIS than those of the Enedis subset. At the IRIS kept in the dataset, the estimates of α^H and α^C passed a significance test. The reference REC for the period 1975–2005 used to calculate the change of temperature-sensitive REC is shown in Fig. 10.

Appendix B. Cross-validation method for trained temperature sensitivities

During the present study, for each cell we have 8 years of annual REC as inputs to train the model described in Equation 2. The Leave-One-Out cross-validation method has been used to fit the model and to validate the model's performance. Each time we extract one year out as test and

train the model with the other 7 years' data and get the prediction using the one test data. And this procedure repeats 8 times. After that, the 8 predicted values with the test data are compared to their initial values, which gives us a test R^2 score. Such test is done for all the cells and a significance test is also performed to get the valid cells. A comparison of different linear regression models has been made with this test method and the distribution of related test R^2 scores are shown in Fig. 11.

Appendix C. AC adoption rate initial data

CODA STRATEGIES uses data from UNICLIMA (the professional union bringing together manufacturers and marketers of AC equipment in France) to estimate the national AC adoption rate from 2004 until 2020, including all types of AC equipment (mobile, heat pump). The national AC rates estimated by CODA STRATEGIES are published by ADEME (the French Agency for Ecological Transition) and are consistent with INSEE (for 2017) and EDF (for 2016 and 2019) data (ADEME, CODA STRATEGIES, 2021). At a finer scale, a study from Ecole des Ponts (Daguenet et al., 2021) calculated the regional AC adoption rate for 2019 based on data from Likibu (a house rental search engine) for over 800 households. The national population-weighted AC rate is found to be 22% for 2019, which is consistent with the EDF study and CODA STRATEGIES dataset.

These studies show that the cooling equipment market increase is not constant and has accelerated in recent years (ADEME, CODA STRATEGIES, 2021), resulting in a more geometric overall progression of about 20% per year at the country scale. From these studies, we have regional rates for 2019 only and national rates from 2016 to 2020 from which regional rates from 2011 to 2018 are deduced assuming a spatially homogeneous progression rate. Once estimated, the national rate "population-weighted national average" is deduced from the estimate of the regional rate for the different years and compared to the reference from ADEME (EDF and INSEE). This reconstruction is consistent for 2016–2020.

Appendix D. AC gradual spreading method and optimal number of neighbors

With the historical REC data, around 60% of the cells are estimated with zero current cooling temperature sensitivity (i.e. $\alpha_i^C = 0$). As described in Section 2.3.2, so-called Gradual Spreading is our way of estimating future α^C based on an interpolation assumption of actual values, especially for cells without current α^C. For cells with positive non-null cooling temperature sensitivity, the future cooling temperature sensitivity is assumed to be consistent with the current value (i.e. $(\alpha_i^C)^{GS} = \alpha_i^C > 0$), while for other cells without current α^C, a nearest-neighbor interpolation is performed with the following formula:

$$\left(\alpha_i^C\right)^{GS} = \frac{1}{J}\sum_{j=0}^{J-1}\alpha_j^C.$$

For a studied cell i, all the cells with current non-null sensitivity $\alpha_j^C > 0$ are ordered by the Euclidean distance with the given cell in the plate carrée projection, and J is the number of nearest cells taken into account for the calculation of the average.

This assumption has been tested with the group of cells where α^C are estimated non-null in the first place. During the test, 60% of these cells are selected randomly to become zero, conforming to the actual situation, and are given an estimation with the Gradual Spreading method. Then the estimated values with Gradual Spreading are compared with the model's initial estimation α^C. This process repeats 30 times for each J, and the average test R^2 score as a function of the number of neighbors J is given in Fig. 12. It can be seen clearly that there exists a local similarity: the test R^2 score is larger when $J \in [10,60]$. In our study, the optimal value for J is 25. Despite selecting the optimal number of cells per cluster based on evidence of local similarity through a pre-test, the resulting prediction R^2 score remains low (below 0.23). This uncertainty in the future assumption of the coefficient α^C remains a limitation of the scenario study with the Gradual Spreading approach.

References

ADEME, CODA STRATEGIES, 2021. La climatisation de confort dans les bâtiments résidentiels et tertiaires. Technical Report. ADEME. 110 pages, URL:https://librairie.ademe.fr.

Auffhammer, M., Mansur, E.T., 2014. Measuring climatic impacts on energy consumption: A review of the empirical literature. Energy Econ. 46, 522–530.

Bettignies, Y., Meirelles, J., Fernandez, G., Meinherz, F., Hoekman, P., Bouillard, P., Athanassiadis, A., 2019. The Scale-Dependent Behaviour of Cities: A Cross-Cities Multiscale Driver Analysis of Urban Energy Use. Sustainability 11, 3246. Number: 12 Publisher: Multidisciplinary Digital Publishing Institute.

Bouramdane, A., Tantet, A., Drobinski, P., 2021. Utility-scale pv-battery versus csp-thermal storage in morocco: Storage and cost effect under penetration scenarios. Energies 14.

Branger, F., Giraudet, L.G., Guivarch, C., Quirion, P., 2015. Global sensitivity analysis of an energy-economy model of the residential building sector. Environ. Modelling Softw. 70, 45–54.

Chen, H.C., Han, Q., De Vries, B., 2020. Modeling the spatial relation between urban morphology, land surface temperature and urban energy demand. Sustainable Cities Soc. 60, 102246.

Chen, H.C., Han, Q., de Vries, B., 2020. Urban morphology indicator analyzes for urban energy modeling. Sustainable Cities Soc. 52, 101863.

Cornes, R.C., van der Schrier, G., van den Besselaar, E.J.M., Jones, P.D., 2018. An Ensemble Version of the E-OBS Temperature and Precipitation Data Sets. J. Geophys. Res.: At. 123, 9391–9409. _eprint: https://onlinelibrary.wiley.com/doi/pdf/10.1029/2017JD028200.

Daguenet, C., Gredigui, P., Teixeira Costa, F., Maugenest, M., Pedro Saint Martin, D., Sena Fracaroli, N., 2021. évolution des besoins en chaud et en froid dans le secteur résidentiel.

Damm, A., Köberl, J., Prettenthaler, F., Rogler, N., Töglhofer, C., 2017. Impacts of +2 C global warming on electricity demand in Europe. Climate Services 7, 12–30.

De Felice, M., Alessandri, A., Ruti, P.M., 2013. Electricity demand forecasting over Italy: Potential benefits using numerical weather prediction models. Electric Power Systems Research 104, 71–79.

Drobinski, P., Silva, N.D., Panthou, G., Bastin, S., Muller, C., Ahrens, B., Borga, M., Conte, D., Fosser, G., Giorgi, F., Güttler, I., Kotroni, V., Li, L., Morin, E., Önol, B., Quintana-Segui, P., Romera, R., Torma, C.Z., 2018. Scaling precipitation extremes with temperature in the Mediterranean: past climate assessment and projection in anthropogenic scenarios. Clim. Dyn. 51, 1237–1257.

ECA&D, 2020. E-OBS data access. URL:https://knmi-ecad-assets-prd.s3.amazonaws.com/ensembles/data/Grid_0.1deg_reg_ensemble/tg_ens_mean_0.1deg_reg_v20.0e.nc. Last visited 2021-06-13.

Emenekwe, C.C., Emodi, N.V., 2022. Temperature and Residential Electricity Demand for Heating and Cooling in G7 Economies: A Method of Moments Panel Quantile Regression Approach. Climate 10, 142. Number: 10 Publisher: Multidisciplinary Digital Publishing Institute.

Emodi, N.V., Chaiechi, T., Alam Beg, A.R., 2018. The impact of climate change on electricity demand in Australia. Energy Environ. 29, 1263–1297.

Enedis, 2020. Consommation et thermosensibilité électriques par secteur d'activité à la maille IRIS. URL:https://data.enedis.fr/explore/dataset/consommation-electrique-par-secteur-dactivite-iris/. Last visited 2020-09-30.

EUROSTAT, Heating and cooling degree days - statistics.

Flaounas, E., Drobinski, P., Bastin, S., 2013. Dynamical downscaling of IPSL-CM5 CMIP5 historical simulations over the Mediterranean: benefits on the representation of regional surface winds and cyclogenesis. Clim. Dyn. 40, 2497–2513.

Flaounas, E., Drobinski, P., Bastin, S., Lebeaupin Brossier, C., Borga, M., Vrac, M., Calvet, J.C., Stéfanon, M., 2013. Precipitation and temperature space-time variability and extremes in the mediterranean region: Evaluation of dynamical and statistical downscaling methods. Clim. Dyn. 40.

Frederiks, E., Stenner, K., Hobman, E., 2015. The Socio-Demographic and Psychological Predictors of Residential Energy Consumption: A Comprehensive Review. Energies 8, 573–609.

Frei, C., Christensen, J.H., Déqué, M., Jacob, D., Jones, R.G., Vidale, P.L., 2003. Daily precipitation statistics in regional climate models: Evaluation and intercomparison for the European Alps. J. Geophys. Res.: At. 108. _eprint: https://onlinelibrary.wiley.com/doi/pdf/10.1029/2002JD002287.

Gertler, P.J., Shelef, O., Wolfram, C.D., Fuchs, A., The demand for energy-using assets among the world's rising middle classes. American Economic Review 106, 1366–1401.

Giraudet, L.G., Guivarch, C., Quirion, P., 2012. Exploring the potential for energy conservation in French households through hybrid modeling. Energy Economics 34, 426–445.

Hallegatte, S., Hourcade, J., Ambrosi, P., 2007. Using climate analogues for assessing climate change economic impacts in urban areas. Climatic Change 82, 47–60.

Haylock, M.R., Goodess, C.M., 2004. Interannual variability of European extreme winter rainfall and links with mean large-scale circulation. Int. J. Climatol. 24, 759–776.

Haylock, M.R., Hofstra, N., Klein Tank, A.M.G., Klok, E.J., Jones, P.D., New, M., 2008. A European daily high-resolution gridded data set of surface temperature and precipitation for 1950–2006. J. Geophys. Res.: At. 113. _eprint: https://onlinelibrary.wiley.com/doi/pdf/10.1029/2008JD010201.

He, P., Liu, P., Qiu, Y.L., Liu, L., 2009. The weather affects air conditioner purchases to fill the energy efficiency gap. Nature Communications 13, 5772. Number: 1 Publisher: Nature Publishing Group.

IGN, 2009. Contours...Iris - Descriptif de contenu et de livraison. Technical Report. Institut Géographique National. URL:https://geoservices.ign.fr/sites/default/files/2022-03/DC_DL_Contours_Iris_09.pdf.

International Energy Agency, Cooling degree days in France, 2000–2020 - Charts - Data & Statistics.

International Energy Agency, 2018. The Future of Cooling.

Jacob, D., Petersen, J., Eggert, B., Alias, A., Christensen, O.B., Bouwer, L.M., Braun, A., Colette, A., Déqué, M., Georgievski, G., Georgopoulou, E., Gobiet, A., Menut, L., Nikulin, G., Haensler, A., Hempelmann, N., Jones, C., Keuler, K., Kovats, S., Kröner, N., Kotlarski, S., Kriegsmann, A., Martin, E., van Meijgaard, E., Moseley, C., Pfeifer, S., Preuschmann, S., Radermacher, C., Radtke, K., Rechid, D., Rounsevell, M., Samuelsson, P., Somot, S., Soussana, J.F., Teichmann, C., Valentini, R., Vautard, R., Weber, B., Yiou, P., 2014. EURO-CORDEX: new high-resolution climate change projections for European impact research. Reg. Environ. Change 14, 563–578.

Kennedy, C.A., Stewart, I., Facchini, A., Cersosimo, I., Mele, R., Chen, B., Uda, M., Kansal, A., Chiu, A., Kim, K.g., Dubeux, C., Rovere, E.L.L., Cunha, B., Pincetl, S., Keirstead, J., Barles, S., Pusaka, S., Gunawan, J., Adegbile, M., Nazariha, M., Hoque, S., Marcotullio, P.J., Otharán, F.G., Genena, T., Ibrahim, N., Farooqui, R., Cervantes, G., Sahin, A.D., 2015. Energy and material flows of megacities. Proceedings of the National Academy of Sciences 112, 5985.

Kjellström, E., Boberg, F., Castro, M., Christensen, J., Nikulin, G., Sanchez, E., 2010. Daily and monthly temperature and precipitation statistics as performance indicators for regional climate models. Climate Res. 44, 135–150.

Klok, E.J., Klein Tank, A.M.G., 2009. Updated and extended European dataset of daily climate observations. Int. J. Climatol. 29, 1182–1191.

Köppen, W., 1936. Das geographische system der klimate, 46 pp.

Kozarcanin, S., Andresen, G.B., Staffell, I., 2019. Estimating country-specific space heating threshold temperatures from national gas and electricity consumption data. Energy and Buildings 199, 368–380.

Larsen, M., Petrovic, S., Radoszynski, A., McKenna, R., Balyk, O., 2020. Climate change impacts on trends and extremes in future heating and cooling demands over Europe. Energy and Buildings 226, 110397.

Lemonsu, A., Viguié, V., Daniel, M., Masson, V., 2015. Vulnerability to heat waves: Impact of urban expansion scenarios on urban heat island and heat stress in Paris (France). Urban Climate 14, 586–605.

Li, H., Kwan, M.P., 2018. Advancing analytical methods for urban metabolism studies. Resour. Conserv. Recycl. 132, 239–245.

Lévy, J.P., Belaïd, F., 2018. The determinants of domestic energy consumption in France: Energy modes, habitat, households and life cycles. Renew. Sustain. Energy Rev. 81, 2104–2114.

Meng, Q., Xiong, C., Mourshed, M., Wu, M., Ren, X., Wang, W., Li, Y., Song, H., 2020. Change-point multivariable quantile regression to explore effect of weather variables on building energy consumption and estimate base temperature range. Sustainable Cities Soc. 53, 101900.

Moral-Carcedo, J., Vicéns-Otero, J., 2005. Modelling the non-linear response of Spanish electricity demand to temperature variations. Energy Economics 27, 477–494.

Narayan, P.K., Smyth, R., Prasad, A., 2007. Electricity consumption in G7 countries: A panel cointegration analysis of residential demand elasticities. Energy Policy 35, 4485–4494.

Pagliarini, G., Bonfiglio, C., Vocale, P., 2019. Outdoor temperature sensitivity of electricity consumption for space heating and cooling: An application to the city of Milan. North of Italy. Energy and Buildings 204, 109512.

Petrick, S., Rehdanz, K., Tol, R., 2010. The Impact of Temperature Changes on Residential Energy Consumption. Kiel Institute for the World Economy, Kiel Working Papers.

Pickett, S.T.A., Cadenasso, M.L., Rosi-Marshall, E.J., Belt, K.T., Groffman, P.M., Grove, J. M., Irwin, E.G., Kaushal, S.S., LaDeau, S.L., Nilon, C.H., Swan, C.M., Warren, P.S., 2017. Dynamic heterogeneity: a framework to promote ecological integration and hypothesis generation in urban systems. Urban Ecosyst. 20, 1–14.

Pilli-Sihvola, K., Remes, P., Ollikainen, M., Tuomenvirta, H., 2010. Climate change and electricity consumption–witnessing increasing or decreasing use and costs? Energy Policy 38, 2409–2419.

Rawat, M., Singh, R.N., 2022. A study on the comparative review of cool roof thermal performance in various regions. Energy and Built Environment 3, 327–347.

Raymond, F., Ullmann, A., Camberlin, P., Drobinski, P., Smith, C.C., 2016. Extreme dry spell detection and climatology over the Mediterranean Basin during the wet season. Geophys. Res. Lett. 43, 7196–7204. _eprint: https://onlinelibrary.wiley.com/doi/pdf/10.1002/2016GL069758.

Raymond, F., Ullmann, A., Camberlin, P., Oueslati, B., Drobinski, P., 2018. Atmospheric conditions and weather regimes associated with extreme winter dry spells over the Mediterranean basin. Clim. Dyn. 50, 4437–4453.

Ribes, A., Boé, J., Qasmi, S., Dubuisson, B., Douville, H., Terray, L., 2022. An updated assessment of past and future warming over france based on a regional observational constraint. Earth Syst. Dyn. 13, 1397–1415.

Rosales Carreón, J., Worrell, E., 2018. Urban energy systems within the transition to sustainable development. A research agenda for urban metabolism. Resour. Conserv. Recycl. 132, 258–266.

van Ruijven, B.J., De Cian, E., Sue Wing, I., 2019. Amplification of future energy demand growth due to climate change. Nat Commun 10, 2762. Number: 1 Publisher: Nature Publishing Group.

Ruti, P.M., Somot, S., Giorgi, F., Dubois, C., Flaounas, E., Obermann, A., Dell'Aquila, A., Pisacane, G., Harzallah, A., Lombardi, E., Ahrens, B., Akhtar, N., Alias, A., Arsouze, T., Aznar, R., Bastin, S., Bartholy, J., Béranger, K., Beuvier, J., Bouffies-Cloché, S., Brauch, J., Cabos, W., Calmanti, S., Calvet, J.C., Carillo, A., Conte, D., Coppola, E., Djurdjevic, V., Drobinski, P., Elizalde-Arellano, A., Gaertner, M., Galàn, P., Gallardo, C., Gualdi, S., Goncalves, M., Jorba, O., Jordà, G., L'Heveder, B., Lebeaupin-Brossier, C., Li, L., Liguori, G., Lionello, P., Maciàs, D., Nabat, P., Önol, B., Raikovic, B., Ramage, K., Sevault, F., Sannino, G., Struglia, M.V., Sanna, A., Torma, C., Vervatis, V., 2016. Med-CORDEX Initiative for Mediterranean Climate Studies. Bulletin of the American Meteorological Society 97, 1187–1208. Publisher: American Meteorological Society Section: Bulletin of the American Meteorological Society.

Räisänen, J., Hansson, U., Ullerstig, A., Döscher, R., Graham, L.P., Jones, C., Meier, H.E. M., Samuelsson, P., Willén, U., 2004. European climate in the late twenty-first century: regional simulations with two driving global models and two forcing scenarios. Clim. Dyn. 22, 13–31.

Sailor, D.J., Muñoz, J.R., 1997. Sensitivity of electricity and natural gas consumption to climate in the U.S.A.–Methodology and results for eight states. Energy 22, 987–998.

Santos, J.A., Corte-Real, J., Ulbrich, U., Palutikof, J., 2007. European winter precipitation extremes and large-scale circulation: a coupled model and its scenarios. Theor. Appl. Climatol. 87, 85–102.

Scapin, S., Apadula, F., Brunetti, M., Maugeri, M., 2016. High-resolution temperature fields to evaluate the response of Italian electricity demand to meteorological variables: an example of climate service for the energy sector. Theor. Appl. Climatol. 125, 729–742.

Spinoni, J., Vogt, J.V., Barbosa, P., Dosio, A., McCormick, N., Bigano, A., Füssel, H.M., 2018. Changes of heating and cooling degree-days in Europe from 1981 to 2100. Int. J. Climatol. 38, e191–e208. _eprint: https://onlinelibrary.wiley.com/doi/pdf/10.1002/joc.5362.

Stefanon, M., D'Andrea, F., Drobinski, P., 2012. Heatwave classification over Europe and the Mediterranean region. Environ. Res. Lett. 7, 014023. Publisher: IOP Publishing.

Stéfanon, M., Drobinski, P., D'Andrea, F., Lebeaupin-Brossier, C., Bastin, S., 2014. Soil moisture-temperature feedbacks at meso-scale during summer heat waves over Western Europe. Clim Dyn 42, 1309–1324.

Tantet, A., Stéfanon, M., Drobinski, P., Badosa, J., Concettini, S., Cretí, A., D'Ambrosio, C., Thomopulos, D., Tankov, P., 2019. e4clim 1.0: The Energy for a Climate Integrated Model: Description and Application to Italy. Energies 12, 4299.

Vaittinada Ayar, P., Vrac, M., Bastin, S., Carreau, J., Déqué, M., Gallardo, C., 2016. Intercomparison of statistical and dynamical downscaling models under the EURO- and MED-CORDEX initiative framework: present climate evaluations. Clim Dyn 46, 1301–1329.

Viguié, V., Lemonsu, A., Hallegatte, S., Beaulant, A.L., Marchadier, C., Masson, V., Pigeon, G., Salagnac, J.L., 2020. Early adaptation to heat waves and future reduction of air-conditioning energy use in Paris. Environ. Res. Lett. 15, 075006. Publisher: IOP Publishing.

Voskamp, I.M., Sutton, N.B., Stremke, S., Rijnaarts, H.H.M., 2020. A systematic review of factors influencing spatiotemporal variability in urban water and energy consumption. J. Cleaner Prod. 256, 120310.

Wenz, L., Levermann, A., Auffhammer, M., 2017. North-south polarization of European electricity consumption under future warming. Proceedings of the National Academy of Sciences 114, 201704339.

Wiedenhofer, D., Lenzen, M., Steinberger, J.K., 2013. Energy requirements of consumption: Urban form, climatic and socio-economic factors, rebounds and their policy implications. Energy Policy 63, 696–707.

You, Y., Kim, S., 2018. Revealing the mechanism of urban morphology affecting residential energy efficiency in Seoul, Korea. Sustainable Cities Soc. 43, 176–190.